virus infection, can be experimentally reproduced in transgenic mice,[30] suggesting that skeletal muscle injury stimulates retrograde axonal transport of poliovirus and thereby facilitates viral invasion of the CNS, resulting in spinal cord damage. These findings afford renewed interest in studying the neural pathway of poliovirus.

Experiments involving transection of the sciatic nerve after IM-inoculation of poliovirus into the calves of PVR-Tg mice revealed that some of the inoculated viruses move along an axon via retrograde transport at a rate of more than 12 cm per day[26] (Fig. 8). This velocity is classified into fast retrograde axonal transport.[31] This suggests that poliovirus is packed in endosomes during transportation through the axon because many substances that are carried retrogradely by the fast transport system are usually packed in endosomes. Indeed, an electron microscopic study detected such endosomes containing poliovirus at synapses in the vicinity of inoculation points.[32] Thus, it is possible that poliovirus is enclosed by endosomes that result from hPVR-mediated endocytosis of the virus at synapses, and then conveyed through the axon retrogradely.

The involvement of hPVR in poliovirus pathogenesis via the neural pathway suggested that poliovirus-related materials in the sciatic nerve are conformationally altered poliovirus (135S and 80S particles) and not 160S virion particles. However, the majority of poliovirus-related materials in the sciatic nerve showed a sedimentation coefficient of 160S[26] (Fig. 9), and the 160S fraction was infectious in cultured cells of primate origin. It is not known, to date, why hPVR-mediated conformational change does not occur for poliovirus-related particles in the sciatic nerve. Possibly, a small number of hPVR per virion is not sufficient to result in viral conformational change but is able to induce endocytosis of the virus on the surface of synapses. Alternatively, a cellular factor(s) that inhibits viral uncoating could exist in the neural pathway of transgenic mice. If this is the case, the virus would require to be free from such a factor(s) before replicating in the neural cell body.

It has been reported that a human homolog (TCTEL1) of mouse Tctex-1, which is light chain-1 of the cytoplasmic dynein complex, binds the cytoplasmic domain of hPVRs,[32),33] and that treatment of the sciatic nerve with the microtubule-depolymerizing agent vinblastin results in slower retrograde transport of the virus to the spinal cord of transgenic mice.[32] Taking into consideration all the observations mentioned above, a possible mechanism for the retrograde axonal transport is shown in Fig. 10. IM-inoculated poliovirus is possibly incorporated into cells by hPVR-mediated endocytosis at synapses without any hPVR-mediated conformational changes of the virion particle. The cytoplasmic domain of hPVR on the surface of endosomes that enclosed the poliovirion could interact with cytoplasmic dynein, and the endosomes could be retrogradely transported along microtubules through the axon to the neuron cell body where uncoating and replication of poliovirus occurs.

A reconstitution of the experimental system was established to support the above hypothesis, in which rat primary neurons were employed. Molecular imaging experiments indicated that endosomes carrying both poliovirus and hPVR move retrogradely through the axon of the primary neurons (S. Ohka *et al.*, manuscript in preparation). However, much research is required to elucidate the mechanisms underlying the endocytosis of poliovirus at synapses and the manner and place where poliovirus replication begins in the neuron cell body. The efficiency of the neural dissemination of poliovirus has been compared between the virulent Mahoney and the attenuated Sabin 1 strains. The data suggest that the difference in efficiency is not significant.[26]

Neurovirulence determinant

The difference in efficiency in the 2 dissemination routes (BBB permeation and retrograde axonal transport) was not observed between the virulent and attenuated poliovirus strains. Thus, the efficiency cannot be a distinct determinant for the expression of strain-specific poliovirus neurovirulence. Thus, strain-specific neurovirulence levels appear to depend primarily on the replication ability of the virus in the CNS.

Comparative sequence analysis between the attenuated Sabin 3 and its neurovirulent revertants revealed an effective mutation of neurovirulence phenotype at nucleotide position 472.[34] Molecular genetic analysis employing reverse genetics of poliovirus type 1 revealed that a relatively strong determinant of neurovirulence resides in the 5′ non-

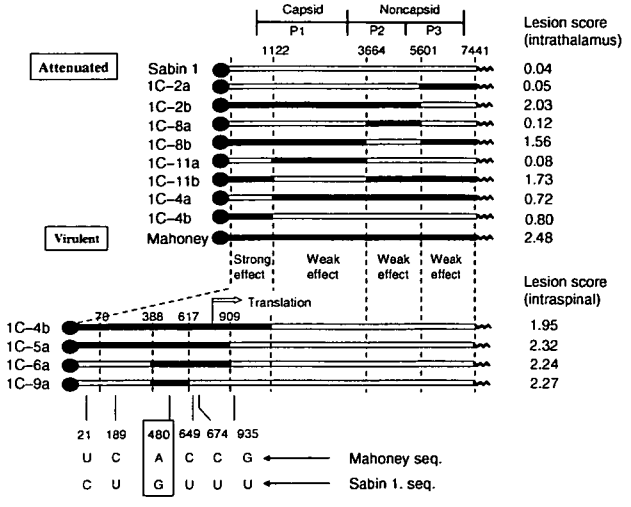

Fig. 11. Genome structure of recombinant type 1 polioviruses. The expected genome structures of the recombinant viruses are shown as a combination of the Sabin 1 (open boxes) and Mahoney (closed boxes) sequences. The numbers over the genome RNAs are the nucleotide positions from the 5′ end of the genome. Nucleotide differences between the Mahoney and Sabin 1 strains are shown at the bottom of the figure. A small protein VPg is indicated by closed circles at the 5′ end of the genomes. Lesion scores obtained from monkey neurovirulence tests are shown on the right of the corresponding genome RNAs. (modified from refs. 35 and 36).

coding sequence of the viral RNA, particularly at nucleotide position 480[35),36)] (Fig. 11). A neurovirulence determinant in the poliovirus type 2 genome has also been investigated, and nucleotide position 481 has been found to be an important nucleotide for this phenotype.

These nucleotide positions exist within the region corresponding to the IRES.[11)] These results suggest that the neurovirulence levels of individual poliovirus strains reflect their IRES activities; that is, the capability of translation initiation activity in the CNS. Although there are multiple neurovirulence determinants on the poliovirus RNA genome, it is interesting that the IRES regions regulate the CNS specificity of the virus. The cumulative evidences offered by the data obtained thus far[38)–40)] led us to the notion of "IRES-dependent virus tropism." In fact, a chimeric poliovirus in which poliovirus IRES is replaced by hepatitis C virus IRES lost the ability to propagate in the brain of transgenic mice but it can grow in the liver.[41)] Thus, the structure and function of the poliovirus IRES should be elucidated for a better understanding of poliovirus pathogenesis.

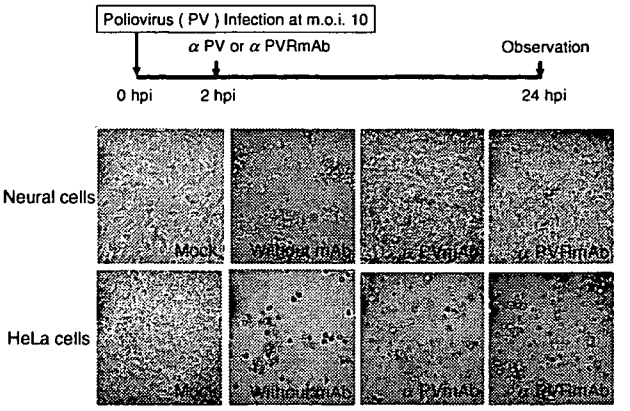

Fig. 12. Inhibition of the poliovirus-induced cytopathic effect in neural cells by mAb against poliovirus or hPVR. Neural cells (upper panels) or HeLa cells (lower panels) were infected with poliovirus type 1 Mahoney strain at an m.o.i. of 10. At 2hpi, the cells were washed three times. Then, medium with or without mAb against poliovirus or hPVR was added to the culture. Poliovirus-infected or mock-infected cells were observed 24 hpi by microscope. (modified from ref. 43).

Anti-poliovirus response of neural cells

It has been reported that post-infection treatment with anti-poliovirus serum results in the survival of neural cells productively infected with virulent poliovirus.[42)] This phenomenon is specific for neural cells but has not been observed in other cells such as HeLa cells. Therefore, this observation might partially reflect *in vivo* pathogenesis of poliovirus specific to neural cells. This phenomenon has been reproduced using mAbs to poliovirus and hPVR instead of anti-poliovirus serum[43)] (Fig. 12). These results indicate that a second infection of neural cells with progeny poliovirus is required for the cells to express cytopathic effects. The reason why cytopathic effects in neural cells are blocked by prevention of the second infection is presently unknown. However, it is possible that the response of neural cells to the first poliovirus infection includes the expression of some cellular factors that inhibit poliovirus IRES activity. In fact, in the presence of mAbs to poliovirus or hPVR, poliovirus-specific protein synthesis was detected by 5 hours post infection (hpi) but not 7 hpi.[43)] In any event, this observation in infected neural cells *in vitro* is consistent with observations in an early study conducted by Bodian.[44)] Moreover, the reason why the second infection induces cytopathic effects in neural cells is totally unknown. Much research

remains to be done to gain insights into the mechanisms of poliovirus neurovirulence.

Acknowledgments

This review is a summary of my scientific achievements on molecular pathogenesis of poliovirus that have been carried out in the State University of New York at Stony Brook, Kitasato University, Tokyo Metropolitan Institute of Medical Science, and The University of Tokyo. I am grateful to so many collaborators on this work since 1974. I thank Etsuko Suzuki in preparing the manuscript and Seii Ohka in drawing Figures.

This work was supported in part by Grants-in-Aid for Specially Promoted Research from the Ministry of Education, Culture, Sports, Science, and Technology of Japan.

References

1) Mendelsohn, C.L., Wimmer, E. and Racaniello, V.R. (1989) Cellular receptor for poliovirus: molecular cloning, nucleotide sequence, and expression of a new member of the immunoglobulin superfamily. Cell **56**, 855–865.
2) Koike, S., Horie, H., Ise, I., Okitsu, A., Yoshida, M., Iiizuka, N., Takeuchi, K., Takegami, T. and Nomoto, A. (1990) The poliovirus receptor protein is produced both as membrane-bound and secreted forms. EMBO J. **9**, 3217–3224.
3) Ren, R., Constantini, F., Gorgacz, E.J., Lee, J.J. and Racaniello, V.R. (1990) Transgenic mice expressing a human poliovirus receptor: a new model for poliomyelitis. Cell **63**, 353–362.
4) Koike, S., Taya, C., Kurata, T., Abe, S., Ise, I., Yonekawa, H. and Nomoto, A. (1991) Transgenic mice susceptible to poliovirus. Proc. Natl. Acad. Sci. USA **88**, 951–955.
5) Bodian, D. (1955) Emerging concept of poliomyelitis infection. Science **122**, 105–108.
6) Sabin, A.B. (1956) Pathogenesis of poliomyelitis: reappraisal in the light of new data. Science **123**, 1151–1157.
7) Hogle, J.M., Chow, M. and Filman, D.J. (1985) Three-dimensional structure of poliovirus at 2.9 Å resolution. Science **229**, 1358–1365.
8) Belnap, D.M., McDermott, B.M. Jr., Filman, D.J., Cheng, N., Trus, B.L., Zuccola, H.J., Racaniello, V.R., Hogle, J.M. and Steven, A.C. (2000) Three-dimensional structure of poliovirus receptor bound to poliovirus. Proc. Natl. Acad. Sci. USA **97**, 73–78.
9) He, Y., Bowman, V.D., Mueller, S., Bator, C.M., Bella, J., Peng, X., Baker, T.S., Wimmer, E., Kuhn, R.J. and Rossmann, M.G. (2000) Interaction of the poliovirus receptor with poliovirus. Proc. Natl. Acad. Sci. USA **97**, 79–84.
10) Xing, L., Tjarnlund, K., Lindqvist, B., Kaplan, G.G., Feigelstock, D., Cheng, R.H. and Casasnovas, J.M. (2000) Distinct cellular receptor interactions in poliovirus and rhinoviruses. EMBO J. **19**, 1207–1216.
11) Pelletier, J. and Sonenberg, N. (1988) Internal initiation of translation of eukaryotic mRNA directed by a sequence derived from poliovirus RNA. Nature **334**, 320–325.
12) Sabin, A.B. and Boulger, L.R. (1973) History of Sabin attenuated poliovirus oral live vaccine strains. J. Biol. Stand. **1**, 115–118.
13) Koike, S., Ise, I. and Nomoto, A. (1991) Functional domains of the poliovirus receptor. Proc. Natl. Acad. Sci. USA **88**, 4104–4108.
14) Selinca, H.-C., Zibert, A. and Wimmer, E. (1991) Poliovirus can enter and infect mammalian cells by way of an intercellular adhesion molecule 1 pathway. Proc. Natl. Acad. Sci. USA **88**, 3598–3602.
15) Morrison, M.E., He, Y.-J., Wien, M.W., Hogle, J.M. and Racaniello, V.R. (1994) Homolog-scanning mutagenesis reveals poliovirus receptor residues important for virus binding and replication. J. Virol. **68**, 2578–2588.
16) Aoki, J., Koike, S., Ise, I., Sato-Yoshida, Y. and Nomoto, A. (1994) Amino acid residues on human poliovirus receptor involved in interaction with poliovirus. J. Biol. Chem. **269**, 8431–8438.
17) Bottino, C., Castriconi, R., Pende, D, Rivera, P., Nanni, M., Carnemolla, B., Cantoni, C., Grassi, J., Marcenaro, S., Reymond, N. *et al.* (2003) Identification of PVR (CD155) and Nectin-2 (CD112) as cell surface ligands for the human DNAM-1 (CD226) activating molecule. J. Exp. Med. **198**, 557–567.
18) Fuchs, A., Cella, M., Giurisato, E., Shaw, A.S. and Colonna, M. (2004) Cutting edge: CD96 (tactile) promotes NK cell-target cell adhesion by interacting with the poliovirus receptor (CD155). J. Immunol. **172**, 3994–3998.
19) Arita, M., Koike, S., Aoki, J., Horie, H. and Nomoto, A. (1998) Interaction of poliovirus with its purified receptor and conformational alteration in the virion. J. Virol. **72**, 3578–3586.
20) Gomez-Yafal, A., Kaplan, G., Racaniello, V.R. and Hogle, J.M. (1993) Characterization of poliovirus conformational alteration mediated by soluble cell receptors. Virology **197**, 501–505.
21) Gromeier, M. and Wetz, K. (1990) Kinetics of poliovirus uncoating in HeLa cells in a nonacidic environment. J. Virol. **64**, 3590–3597.
22) Ren, R. and Racaniello, V.R. (1992) Human poliovirus receptor gene expression and poliovirus tissue tropism in transgenic mice. J. Virol. **66**, 296–304.
23) Abe, S., Ota, Y., Koike, S., Kurata, T., Horie, H., Nomura, T., Hashizume, S. and Nomoto, A. (1995) Neurovirulence test for oral live poliovaccines using poliovirus-sensitive transgenic mice. Virology **206**, 1075–1083.
24) Horie, H., Koike, S., Kurata, T., Sato-Yoshida, Y., Ise, I., Ota, Y., Abe, S., Hioki, K., Kato, H.,

Taya, C. *et al.* (1994) Transgenic mice carrying the human poliovirus receptor: new animal model for study of poliovirus neurovirulence. J. Virol. **68**, 681–688.
25) Yang, W.-X., Terasaki, T., Shiroki, K., Ohka, S., Aoki, J., Tanabe, S., Nomura, T., Terada, E., Sugiyama, Y. and Nomoto, A. (1997) Efficient delivery of circulating poliovirus to the central nervous system independently of poliovirus receptor. Virology **229**, 421–428.
26) Ohka, S., Yang, W.-X., Terada, E., Iwasaki, K. and Nomoto, A. (1998) Retrograde transport of intact poliovirus through the axon via the fast transport system. Virology **250**, 67–75.
27) Ohka, S., Igarashi, H., Nagata, N., Sakai, M., Koike, S., Nochi, T., Kiyono, H. and Nomoto, A. (2007) Establishment of a poliovirus oral infection system in human poliovirus receptor-expressing transgenic mice that are deficient in alpha/beta interferon receptor. J. Virol. **81**, 7902–7912.
28) Nathanson, N. and Langmuir, A.D. (1963) The Cutter incident: poliomyelitis following from aldehyde-inactivated poliovirus vaccination in the United States during the spring of 1955. III. Comparison of the clinical character of vaccinated and contact cases occurring after use of high rate lots of Cutter vaccine. Am. J. Hyg. **78**, 61–81.
29) Ren, R. and Racaniello, V.R. (1992) Poliovirus spreads from muscle to the central nervous system by neural pathways. J. Infect. Dis. **166**, 747–752.
30) Gromeier, M. and Wimmer, E. (1998) Mechanism of injury-provoked poliomyelitis. J. Virol. **72**, 5056–5060.
31) Brady, S.T. (1991) Molecular motors in the nervous system. Neuron **7**, 521–533.
32) Ohka, S., Matsuda, N., Tohyama, K., Oda, T., Morikawa, M., Kuge, S. and Nomoto, A. (2004) Receptor (CD155)-dependent endocytosis of poliovirus and retrograde axonal transport of the endosome. J. Virol. **78**, 7186–7198.
33) Mueller, S., Cao, X., Welker, R. and Wimmer, E. (2002) Interaction of poliovirus receptor CD155 with the dynein light chain Tctex-1 and its implication for poliovirus pathogenesis. J. Biol. Chem. **277**, 7897–7904.
34) Evans, D.M., Dunn, G., Minor, P.D., Schild, G.C., Cann, A.J., Stanway, G., Almond, J.W., Currey, K. and Maizel, J.V. Jr. (1985) Increased neurovirulence associated with a single nucleotide change in a noncoding region of the Sabin type 3 poliovaccine genome. Nature **314**, 548–550.
35) Omata, T., Kohara, M., Kuge, S., Komatsu, T., Abe, S., Semler, B.L., Kameda, A., Itoh, H., Arita, M., Wimmer, E. and Nomoto, A. (1986) Genetic analysis of the attenuation phenotype of poliovirus type 1. J. Virol. **58**, 348–358.
36) Kawamura, N., Kohara, M., Abe, S., Komatsu, T., Tago, K., Arita, M. and Nomoto, A. (1989) Determinants in the 5′ noncoding region of poliovirus Sabin 1 RNA that influence the attenuation phenotype. J. Virol. **63**, 1302–1309.
37) Macadam, A.J., Pollard, S.R., Ferguson, G., Dunn, G., Skuce, R., Almond, J.W. and Minor, P.D. (1991) The 5′ noncoding region of the type 2 poliovirus vaccine strain contains determinants of attenuation and temperature sensitivity. Virology **181**, 451–458.
38) Shiroki, K., Ishii, T., Aoki, T., Ota, Y., Yang, W.-X., Komatsu, T., Ami, Y., Arita, M., Abe, S., Hashizume, S. and Nomoto, A. (1997) Host range phenotype induced by mutations in the internal ribosomal entry site of poliovirus RNA. J. Virol. **71**, 1–8.
39) Kamoshita, N., Tsukiyama-Kohara, K., Kohara, M. and Nomoto, A. (1997) Genetic analysis of internal ribosomal entry site on hepatitis C virus RNA: implication for involvement of the highly ordered structure and cell type-specific transacting factors. Virology **233**, 9–18.
40) Isoyama, T., Kamoshita, N., Yasui, K., Iwai, A., Shiroki, K., Toyoda, H., Yamada, A., Takasaki, Y. and Nomoto, A. (1999) Lower concentration of La protein required for internal ribosome entry on hepatitis C virus RNA than on poliovirus RNA. J. Gen. Virol. **80**, 2319–2327.
41) Yanagiya, A., Ohka, S., Hashida, N., Okamaura, M., Taya, C., Kamoshita, N., Iwasaki, K., Sasaki, Y., Yonekawa, H. and Nomoto, A. (2003) Tissue specific replicating capacity of a chimeric poliovirus that carries the internal ribosome entry site of hepatitis C virus in a new mouse model transgenic for human poliovirus receptor. J. Virol. **77**, 10479–10487.
42) Tolskaya, E.A., Ivannikova, T.A., Kolesnikova, M.S., Drozdov, S.G. and Agol, V.I. (1992) Postinfection treatment with antiviral serum results in survival of neural cells productively infected with virulent poliovirus. J. Virol. **66**, 5152–5156.
43) Yanagiya, A., Jia, Q., Ohka, S., Horie, H. and Nomoto, A. (2005) Blockade of the poliovirus-induced cytopathic effect in neural cells by monoclonal antibody against poliovirus or the human poliovirus receptor. J. Virol. **79**, 1523–1532.
44) Bodian, D. (1949) Histopathologic basis of clinical findings in poliomyelitis. Am. J. Med. **6**, 563–578.

(Received Aug. 31, 2007; accepted Sept. 25, 2007)

Profile

Akio Nomoto was born in 1946 and started his research career in 1969 with studies on the transfer RNA from baker's yeast, in the Faculty of Pharmaceutical Science, the University of Tokyo, after his graduation from the same faculty. He first encountered poliovirus when he joined Prof. Eckard Wimmer's laboratory, the State University of New York at Stony Brook, as a post-doctoral fellow in 1974. He worked on VPg, which is a small protein attached to the 5′ terminus of all the poliovirus RNAs except for its mRNA. He came back to Japan in 1977 and started as an associate professor at the School of Pharmaceutical Science, Kitasato University, and determined the total genome sequences of all three serotypes of poliovirus Sabin strains. After his moving to the Faculty of Medicine, the University of Tokyo as an associate professor in 1982, he identified the attenuating mutation on the RNA of the Sabin 1 vaccine strain of poliovirus using reverse genetics. This work opened a new avenue for elucidating the molecular mechanisms of the poliovirus pathogenesis. By using the knowledge obtained from above work, he constructed new candidates of type 2 and type 3 oral live vaccine strains by recombinant DNA technology. In 1987, he moved to Department of Microbiology, the Tokyo Metropolitan Institute of Medical Science as a Department Director, and another pioneering work was performed in this Institute, that is, discovery of human poliovirus receptor (hPVR) which determines species-specificity of poliovirus. He and his coworkers generated poliovirus-sensitive mice which were transgenic for hPVR. He was promoted to Professor at the University of Tokyo in 1991 and became Head of the Department of Microbiology at the Institute of Medical Science. Using the transgenic mice, he and his coworkers investigated poliovirus dissemination pathway in a whole body at molecular level, and proved that the transgenic mouse was a very useful animal model for studying molecular pathogenesis of poliovirus. He moved to the Department of Microbiology, Graduate School of Medicine, the University of Tokyo in 2000, where he continues to study poliovirus pathogenesis and is educating many students in the field of microbiology. He was awarded the Hideyo Noguchi Memorial Award for Medical Sciences in 1987, the Naito Foundation Research Prize in 1998, the Takeda Prize for Medical Science in 2002, and the Japan Academy Prize in 2004.

JOURNAL OF VIROLOGY, Feb. 2005, p. 1523–1532 Vol. 79, No. 3
0022-538X/05/$08.00+0 doi:10.1128/JVI.79.3.1523–1532.2005

Blockade of the Poliovirus-Induced Cytopathic Effect in Neural Cells by Monoclonal Antibody against Poliovirus or the Human Poliovirus Receptor

Akiko Yanagiya,[1]† Qingmei Jia,[1]‡ Seii Ohka,[1] Hitoshi Horie,[2] and Akio Nomoto[1]*

Department of Microbiology, Graduate School of Medicine, The University of Tokyo, Hongo, Bunkyo-ku,[1] and Japan Poliomyelitis Research Institute, Kumegawa, Higashimurayama,[2] Tokyo, Japan

Received 20 May 2004/Accepted 19 September 2004

The poliovirus (PV)-induced cytopathic effect (CPE) was blocked in neural cells but not in HeLa cells by the addition of monoclonal antibody (MAb) against PV or the human PV receptor (CD155) 2 h postinfection (hpi). Since each MAb has the ability to block viral infection, no CPE in PV-infected neural cells appeared to result from the blockade of multiple rounds of viral replication. Pulse-labeling experiments revealed that virus-specific protein synthesis proceeded 5 hpi with or without MAbs. However, in contrast to the results obtained without MAbs, virus-specific protein synthesis with MAbs was not detected 7 hpi. Shutoff of host translation was also not observed in the presence of MAbs. Western blot analysis showed that $2A^{pro}$, the viral protein which mediates the cleavage of eukaryotic translation initiation factor eIF4G, was still present 11 hpi. However, intact eIF4G appeared 11 hpi. An immunocytochemical study indicated that $2A^{pro}$ was detected only in the nucleus 11 hpi. These results suggest that neural cells possess protective response mechanisms against PV infection as follows: (i) upon PV infection, neural cells produce a factor(s) to suppress PV internal ribosome entry site activity by 7 hpi, (ii) a factor which supports cap-dependent translation for eIF4G may exist in infected cells when no intact eIF4G is detected, and (iii) the remaining $2A^{pro}$ is not effective in cleaving eIF4G because it is imported into the nucleus by 11 hpi.

Poliovirus (PV), the causative agent of poliomyelitis, is an enterovirus that belongs to the *Picornaviridae*. The genome of PV is a single-stranded, positive-sense RNA of approximately 7.5 kb and functions as mRNA after entry into the host cell cytoplasm. PV mRNA is uncapped and its translation is initiated by binding of the ribosome to viral mRNA downstream of the 5′ end, an RNA structure termed the internal ribosome entry site (IRES) (24, 29). The mRNA has only one long open reading frame encoding the viral polyprotein, which consists of the capsid precursor (P1) and the noncapsid precursors (P2 and P3) (38). The polyprotein is cotranslationally processed by virus-specific proteases $2A^{pro}$ and $3C^{pro}$ ($3CD^{pro}$) to generate mature viral proteins (17, 33). $2A^{pro}$ cleaves a Tyr-Gly bond (13, 19, 28, 36), and $3C^{pro}$ ($3CD^{pro}$) cleaves a Gln-Gly bond.

Upon infection, PV induces the shutoff of almost all host cell translation and induces a severe cytopathic effect (CPE) in infected cells. Both phenomena are thought to be induced mainly by $2A^{pro}$ expression (3). The shutoff of host cell translation has been thought to result from the cleavage of eukaryotic translation initiation factor eIF4G (9, 18, 41) and poly(A) binding protein (34). eIF4G is a subunit of eIF4F, which also contains eIF4E, the cap binding protein, and eIF4A, the RNA helicase (4, 26). eIF4G itself serves as a scaffold protein which interacts with eIF4E and eIF4A, and its association with eIF3 has been suggested to promote attachment of the small ribosomal subunit at the 5′ ends of mRNAs (4, 26, 30). The cleavage of eIF4G blocks the formation of the cap-dependent translation complex, leading to the shutoff of host translation (10, 16, 20). Contrary to cap-dependent translation, the C-terminal cleavage product of eIF4G is sufficient to carry out IRES-dependent translation, and the synthesis of viral polyprotein continues after eIF4G cleavage (4, 8, 10, 12, 18, 41).

PV-infected cells show typical signs of the CPE, such as rounding up, accumulation of membranous vesicles (5, 7), condensation of chromatin (6), and detachment from the basal surface of culture dishes. Furthermore, a number of host nuclear proteins are redistributed from the nucleus to the cytoplasm during PV infection (23, 25, 32, 37). In addition, some components of the nuclear pore complex are degraded during PV infection (11). However, little is known about the molecular mechanisms responsible for CPE expression due to PV infection.

Tolskaya et al. (35) reported that the CPE in human neuroblastoma cells infected with virulent PV is suppressed by the addition of anti-PV hyperimmune serum shortly after the infection. They argued that the antibodies penetrate the cells, interact with assembled viral particles, and inhibit an unknown reaction responsible for cell death. Here we describe a similar observation obtained with an anti-human PV receptor (hPVR; CD155) monoclonal antibody (MAb) as well as an anti-PV MAb. Both MAbs have the ability to block PV infection. Thus, a new concept that elucidates the mechanisms responsible for this phenomenon is desirable. Our biochemical and immunocytochemical studies suggest the existence of specific mecha-

* Corresponding author. Mailing address: Department of Microbiology, Graduate School of Medicine, The University of Tokyo, 7-3-1 Hongo, Bunkyo-ku, Tokyo 113-0033, Japan. Phone: 81-3-5841-3413. Fax: 81-3-5841-3374. E-mail: anomoto@m.u-tokyo.ac.jp.

† Present address: Department of Biochemistry, McGill University, McIntyre Medical Sciences Building, Rm. 807, 3655 Drummond St., Montreal, Quebec, Canada H3G 1Y6.

‡ Present address: Department of Molecular and Medical Pharmacology, CHS 23-120, University of California at Los Angeles, Los Angeles, CA 90095.

nisms that produce a protective response against PV infection in neural cells.

MATERIALS AND METHODS

Cells and viruses. Human neuroblastoma cell lines SK-N-SH and IMR-32 were maintained in Dulbecco modified Eagle medium (DMEM) supplemented with 10% fetal calf serum. African green monkey kidney (AGMK) cells and HeLa S3 monolayer cells were maintained in DMEM supplemented with 5% newborn calf serum. AGMK cells were used for transfection and virus titration experiments. The Mahoney strain of PV type 1 (PV1/Mahoney) and a mutant PV (2A-HA virus) expressing hemagglutinin (HA)-tagged $2A^{pro}$ for intact $2A^{pro}$ were produced in AGMK cells transfected with the corresponding RNAs transcribed in vitro from infectious cDNA clones of pOM1 (31) and p2A-HA (an infectious cDNA clone of 2A-HA virus; see below), respectively. Cells transfected with RNA transcribed from pOM1 or p2A-HA were incubated in DMEM containing 5% newborn calf serum at 37°C for up to 3 days to recover the corresponding virus.

DNA procedures. Infectious cDNA clone pOM1 was used as a template for the construction of p2A-HA, in which the nucleotide sequence for intact $2A^{pro}$ in pOM1 was replaced by sequences encoding $2A^{pro}$, the HA tag, and an artificial $3C^{pro}$ cleavage site, in that order. Silent mutations were introduced into the nucleotide sequence of the artificial $3C^{pro}$ cleavage site to avoid recombination with the authentic nucleotide sequence at the 3′ terminus of the $2A^{pro}$ coding sequence. See Fig. 7 for the genome structure of 2A-HA virus.

To construct a plasmid which expressed only HA-tagged $2A^{pro}$ driven by the PV IRES in transfected cells, nucleotides 108 to 742 of pOM1 and nucleotide sequences encoding methionine, the $2A^{pro}$ cleavage site DLTTY*G (the asterisk denotes a scissile bond), $2A^{pro}$, and the HA tag were joined in frame in that order and inserted into mammalian expression vector pCI-neo (Promega). The resultant expression vector was designated pI108-2A-HA. DOTAP liposomal transfection reagent (Roche) was used for transfection of cells with this expression vector.

Antibodies. Anti-PV1/Mahoney MAb 7m008 and anti-PV1/Sabin MAb 8a034 were kindly provided by the Japan Poliomyelitis Research Institute. MAb 7m008 can neutralize both PV1/Mahoney and PV1/Sabin, and MAb 8a034 is a neutralizing antibody specific for PV1/Sabin but not for PV1/Mahoney. Rabbit anti-PV1/Mahoney hyperimmune serum was prepared by immunizing rabbits with purified PV1/Mahoney. Rabbit polyclonal antibodies against $2A^{pro}$ were prepared by using the C-terminal 14 amino acids of $2A^{pro}$ (IRDLYAYEEEAMEQ) as an antigen. Those against eIF4G were elicited against a peptide of 17 residues (FYSWESSKDPAEQQGKG) corresponding to amino acid residues 37 to 21 of the C terminus of eIF4G. The anti-hPVR MAb (p286) used in this study was able to bind domain 1 of hPVR and block PV infection.

PV infection. SK-N-SH and HeLa cells were infected with PV1/Mahoney or PV1/Sabin at a multiplicity of infection (MOI) of 10. After incubation at 37°C for 30 min, the infected cells were washed with serum-free medium and then incubated in fresh medium at 37°C for 1.5 h. Next, the medium was replaced with fresh medium containing MAb 7m008 (1:10 dilution), MAb 8a034 (1:10 dilution), or MAb p286 (1:3 dilution). Cell morphology was observed 24 hours postinfection (hpi) by light microscopy (Olympus IX70).

To study growth kinetics in a single cycle of infection, PV1/Mahoney-infected cell cultures were subjected to freezing-thawing three times at various times. The virus titers of the supernatants were measured by plaque assays after the removal of cell debris by centrifugation.

Pulse-labeling. Infected cells were washed twice with methionine- and cysteine-free DMEM and incubated in the same medium at 37°C for 30 min. The cells then were supplemented with 100 μCi of [^{35}S]methionine and [^{35}S]cysteine per ml at various times and incubated at 37°C for 30 min. Next, the cells were washed three times with phosphate-buffered saline (PBS; 8 g of NaCl, 0.2 g of KCl, 1.15 g of Na_2HPO_4, and 0.2 g of KH_2PO_4 per liter) and lysed in TSA solution (10 mM Tris-HCl [pH 8.0], 140 mM NaCl, 0.025% NaN_3, 1 mM phenylmethylsulfonyl fluoride, 10 μg of leupeptin/ml, 10 μg of aprotinin/ml) containing 1% Nonidet P-40 (NP-40). After the removal of cell debris by centrifugation, the lysates were separated by 12% polyacrylamide gel electrophoresis (PAGE) in a buffer containing 0.1% sodium dodecyl sulfate. The gels were dried, and the protein bands were visualized by autoradiography.

Northern blot analysis. Infected SK-N-SH cells were treated with MAb p286 2 hpi and collected 7 hpi. They were homogenized in a Dounce homogenizer with PBS containing 1% NP-40 and 0.1% bovine serum albumin (BSA, fraction V; Sigma). After centrifugation to remove cell debris, the supernatants were applied to a 15 to 30% sucrose density gradient in PBS containing 1% NP-40 and 0.1% BSA. Centrifugation was performed at 41,000 rpm for 1 h at 4°C in a Beckman SW55Ti rotor. RNA was extracted from each fraction, treated at 65°C for 15 min in MOPS buffer [20 mM 3-(*N*-morpholino)propanesulfonic acid (MOPS) (pH 7.0), 5 mM CH_3COONa, 1 mM EDTA] containing formaldehyde and formamide, and separated by 1% agarose gel electrophoresis in MOPS buffer. Northern blot analysis was carried out with AlkPhos Direct (Amersham Pharmacia Biotech) in accordance with the manufacturer's instructions. The probe used was negative-strand RNA complementary to nucleotides 1 to 742 of pOM1 to detect only positive-strand PV RNA. An AmpliScribe T3 transcription kit (Epicentre Technologies) was used for in vitro transcription.

Western blot analysis. Infected cells were lysed in TSA solution containing 1% NP-40 at various times. After centrifugation to remove cell debris, the lysates were separated by 15% PAGE to detect $2A^{pro}$ and by 6% PAGE to detect eIF4G in a buffer containing 0.1% sodium dodecyl sulfate. The proteins were transferred to an Immobilon transfer membrane (Millipore), probed with rabbit anti-$2A^{pro}$ antibodies or rabbit anti-eIF4G antibodies, and treated with goat anti-rabbit immunoglobulins conjugated with peroxidase. Protein bands were visualized by using enhanced chemiluminescence detection reagents (Amersham).

Immunofluorescence study. Infected cells were washed once with PBS, fixed with 2% paraformaldehyde at room temperature for 10 min, and washed with PBS. After treatment with PBS containing 100 mM glycine at room temperature for 20 min, the cells were subjected to permeation with PBS containing 0.5% Triton X-100 at 4°C for 5 min and then were washed with PBS. Nonspecific staining was blocked by treatment with 3% BSA and 0.02% NaN_3 in PBS at 37°C for 30 min. The cells were treated with rabbit hyperimmune serum against PV at 37°C for 2 h and then treated with goat anti-rabbit immunoglobulin G conjugated with Alexa Fluor 488 (Molecular Probes) at 37°C for 2 h. Nucleic acids were stained with 4′,6′-diamidino-2-phenylindole. Next, the cells were mounted with 80% (vol/vol) glycerol and analyzed with an inverted microscope (DM IRE2; Leica Microsystems) equipped with a confocal imaging spectrophotometer (TCS SP2; Leica Microsystems).

To detect HA-tagged $2A^{pro}$, a rat anti-HA MAb (Roche) and goat anti-rat immunoglobulin G conjugated with Alexa Fluor 488 were used as primary and secondary antibodies, respectively.

RESULTS

Effect of MAb against PV or the hPVR on the PV-induced CPE. The PV-induced CPE in neural cells is blocked by the addition of rabbit hyperimmune serum against PV 2 hpi (35). To gain insight into the mechanisms responsible for this effect, MAb against PV or the hPVR was used for rabbit hyperimmune serum. SK-N-SH cells infected with PV1/Mahoney at an MOI of 10 showed typical signs of the CPE by 24 hpi without MAb, as expected (Fig. 1B). However, CPE expression was blocked when MAb against PV type 1 (7m008) was added 2 hpi (Fig. 1C). This blockade was not successful with MAb 8a034, a neutralizing MAb specific for PV1/Sabin, an oral poliovaccine strain derived from parental virulent PV1/Mahoney (Fig. 1E). CPE progression in neural cells infected with PV1/Sabin was inhibited by the addition of MAb 7m008 or 8a034 (data not shown). Thus, only neutralizing antibodies were effective in inhibiting CPE expression in neural cells. Neutralizing antibodies may inhibit PV infection before eclipse of the virus, and eclipse of PV by HeLa cells occurs much earlier than 2 hpi, but SK-N-SH cells may differ in that regard (14). This situation may result in efficient blockade of the CPE in PV-infected SK-N-SH cells by the addition of neutralizing antibodies 2 hpi. However, the eclipse scenario is not likely, because the PV generation time in SK-N-SH cells is very similar to that in HeLa cells (Fig. 2).

Similar inhibition was observed with the addition of MAb against hPVR (p286) (Fig. 1D). MAb p286 blocks PV infection by binding to domain 1 of hPVR, which is the PV binding site. This MAb also blocked the CPE induced by PV1/Sabin (data not shown). These results suggest that the inhibition of CPE

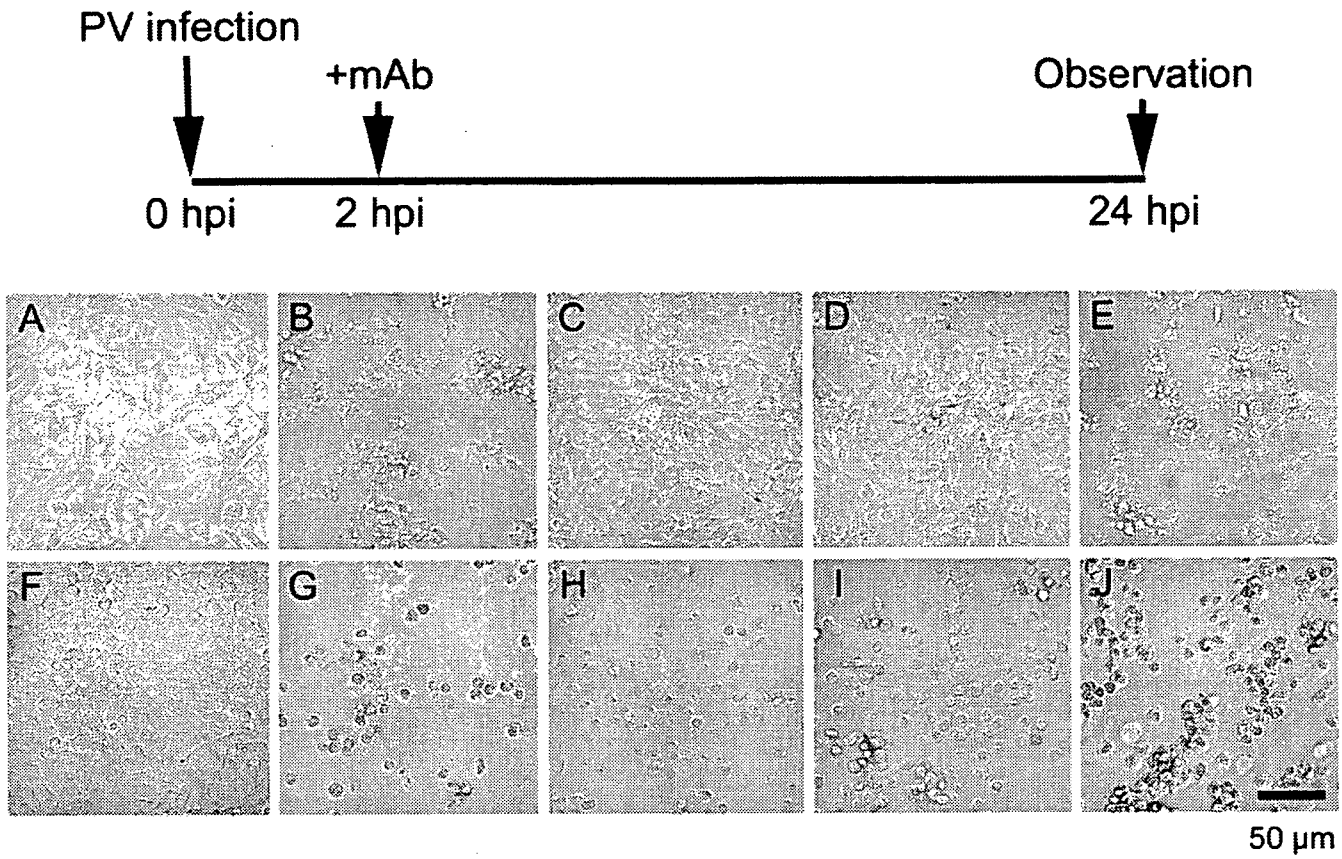

FIG. 1. Inhibition of the PV-induced CPE in neural cells by MAb against PV or hPVR. Neural cells (A, B, C, D, and E) or HeLa cells (F, G, H, I, and J) were infected with PV1/Mahoney at an MOI of 10 (mock infection in panels A and F). At 2 hpi, the cells were washed three times. Then, medium not supplemented with MAbs (A, B, F, and G) or medium supplemented with MAbs against both PV1/Mahoney and PV1/Sabin (C and H), against hPVR (D and I), or against PV1/Sabin (E and J) was added to the culture. PV-infected cells were observed 24 hpi by microscopy.

expression in neural cells is due to the blockade of multiple rounds of viral replication. In fact, efficient CPE blockade by the addition of MAbs disappeared when the MAbs were added later than 5 hpi, the time by which some progeny virions had already been released into the culture medium, as in PV-infected HeLa cells (data not shown). HeLa cells, however, displayed a severe CPE regardless of whether the cells were treated with MAbs or not (Fig. 1G to J).

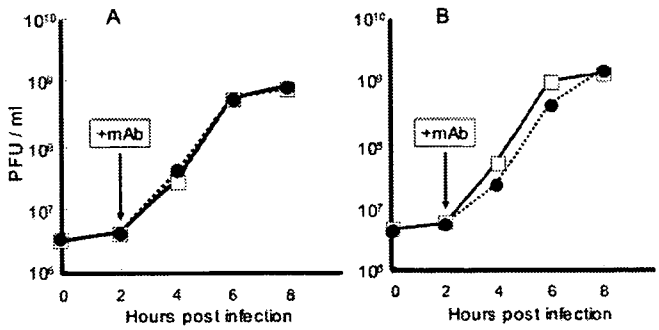

FIG. 2. PV replication in a single cycle of infection with or without MAbs. Virus titers in PV-infected cells at the indicated times were measured as described in Materials and Methods and plotted. SK-N-SH cells (A) and HeLa cells (B) were infected with PV1/Mahoney. The cells were treated with MAb against hPVR (□) or not treated with MAb (●) 2 hpi.

Virus yield with or without MAb. It is possible that virus yield resulting from the lytic replication of PV determines whether or not CPE expression occurs. To test this hypothesis, PV yields in HeLa and SK-N-SH cells were examined in the presence or absence of MAb p286. The time profiles are shown in Fig. 2. The growth rate and final yield for PV1/Mahoney in HeLa and SK-N-SH cells with MAb p286 were almost identical to those without the MAb. Thus, viral replication efficiency is not affected by the addition of MAb in HeLa or SK-N-SH cells. These data indicate that virus yield is not a determinant of CPE expression in this situation. A similar experiment involving MAb 7m008 was not successful due to its neutralizing activity against PV.

Clearance of PV antigens in neural cells. PV-infected neural cells treated with MAbs 2 hpi can be maintained by further passaging. Thus, infected cells are eventually cured of viral infection. It is possible that, after a single cycle of viral replication (Fig. 2), the clearance of PV occurs in infected neural cells. To examine the amounts of PV antigens present in neural cells, PV-infected neural cells in the absence or presence of MAb 7m008 or p286 were examined in an immunofluorescence study 11 and 24 hpi. As shown in Fig. 3, in the absence

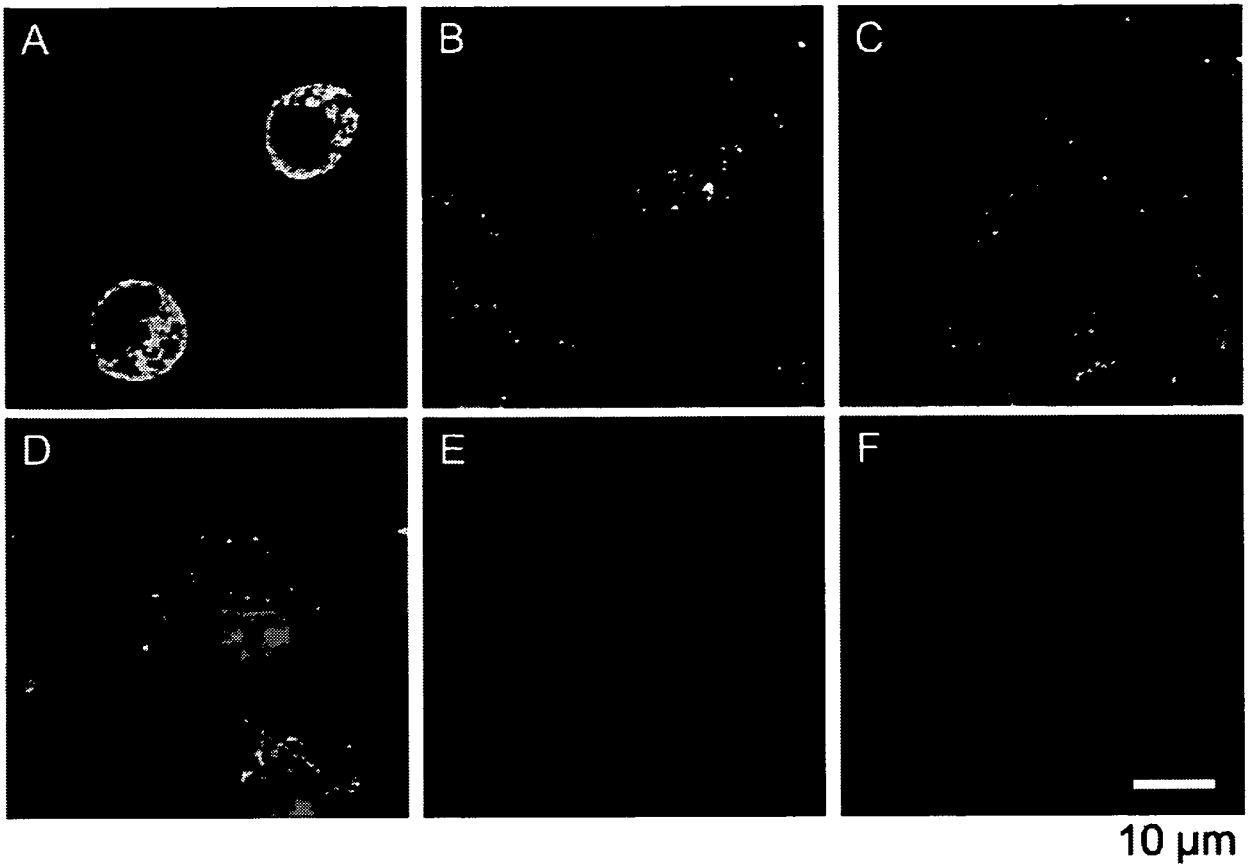

FIG. 3. PV antigens in PV-infected neural cells with or without MAbs. PV-infected cells were examined in an immunofluorescence study 11 hpi (A, B, and C) and 24 hpi (D, E, and F). At 2 hpi the cells were not treated with MAb (A and D) or were treated with MAb against PV (B and E) or against hPVR (C and F). Red indicates nucleic acids, and green indicates PV antigens.

of MAb, neural cells showed a CPE by 11 hpi (Fig. 3A) and were destroyed by 24 hpi (Fig. 3D). They also retained significant amounts of PV antigens. In the presence of MAb, however, the amounts of PV antigens observed 11 hpi (Fig. 3B and C) dramatically decreased by 24 hpi (Fig. 3E and F). These data suggest that neural cells possess a mechanism for eliminating PV antigens with the aid of MAbs.

Protein synthesis in PV-infected neural cells. Pulse-labeling experiments were performed as described in Materials and Methods to examine host and viral protein synthesis in neural cells (Fig. 4A) and HeLa cells (Fig. 4B) at various times after PV infection. In neural cells without MAb, viral protein synthesis was detected by 5 hpi and continued until at least 11 hpi, when the shutoff of host translation was observed (Fig. 4A) and the cells displayed a CPE (Fig. 3A). In the presence of MAb 7m008 or p286, however, PV-specific protein synthesis was detected by 5 hpi but not at 7 hpi (Fig. 4A), and host translation continued to occur (Fig. 4A). In HeLa cells (Fig. 4B), the shutoff of host translation was evident by 5 hpi, and PV-specific protein synthesis continued until at least 7 hpi regardless of whether the cells were treated with MAbs or not. These data also indicate that neural cells possess a mechanism that provides protection against PV infection.

It is possible that the inhibition of PV-specific protein synthesis was due to the degradation of PV mRNA in neural cells between 5 and 7 hpi. To exclude this possibility, a PV-infected neural cell culture was treated with MAb p286 2 hpi and harvested 7 hpi, and the cell extract was subjected to sucrose density gradient centrifugation to separate PV mRNA and PV virion particles. Northern blot analysis was carried out to detect the positive-sense PV RNA in each fraction (Fig. 5). The results indicate that a significant amount of free positive-sense PV RNA (PV mRNA) was present in the cell extract. These data suggest that PV-specific protein synthesis was inhibited at a stage of translation, that is, PV IRES activity was inhibited, although it is not known at present whether the antibody treatment also affected PV-specific RNA synthesis. It is possible that neural cells produce a factor(s) that inhibits PV IRES activity in response to PV infection in the presence of MAb.

Existence of $2A^{pro}$ in PV-infected neural cells. Among PV-specific proteins, $2A^{pro}$ is thought to be the most important viral molecule for inducing the CPE and host translation shutoff in infected cells. Accordingly, the existence of $2A^{pro}$ in PV-infected neural cells was examined by Western blot analysis. As shown in Fig. 6A, the maximum amount of $2A^{pro}$ was detected 5 hpi with or without MAb. The amount of $2A^{pro}$ detected 11 hpi was similar to that detected 5 hpi in the absence of MAb. However, the amount of $2A^{pro}$ decreased by 11 hpi in the presence of MAb. This result was expected because PV-specific protein synthesis was inhibited by 7 hpi (Fig. 4A).

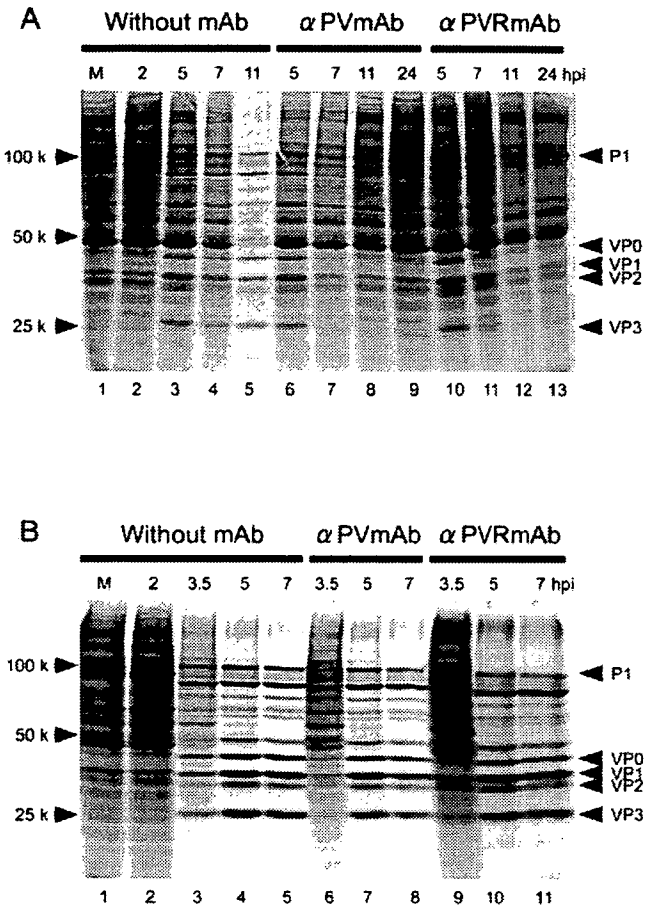

FIG. 4. Protein synthesis in PV-infected cells. Protein synthesis in PV-infected cells was investigated by a pulse-labeling assay with [^{35}S]methionine. M (lane 1), mock infection. Neural cells (A) or HeLa cells (B) were pulse-labeled for 30 min beginning at the indicated times. Neural cells were not treated 2 hpi with MAb (lanes 2 to 5) or were treated 2 hpi with MAb against PV (lanes 6 to 9) or against hPVR (lanes 10 to 13). HeLa cells were not treated 2 hpi with MAb (lanes 2 to 5) or were treated 2 hpi with MAb against PV (lanes 6 to 8) or against hPVR (lanes 9 to 11).

The turnover of 2A^{pro} was probably not complete by 11 hpi but appeared to be complete by 24 hpi. In the absence of MAb, only a small amount of 2A^{pro} was detected 24 hpi because many cells had been destroyed or were detached (Fig. 3D). In

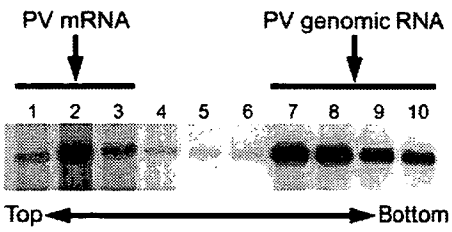

FIG. 5. Detection of PV mRNA. PV-infected neural cells treated with MAb against hPVR 2 hpi were collected 7 hpi and homogenized. The supernatants of the homogenates were analyzed by sucrose density gradient centrifugation as described in Materials and Methods. Total RNA was extracted from each fraction and subjected to Northern blot analysis.

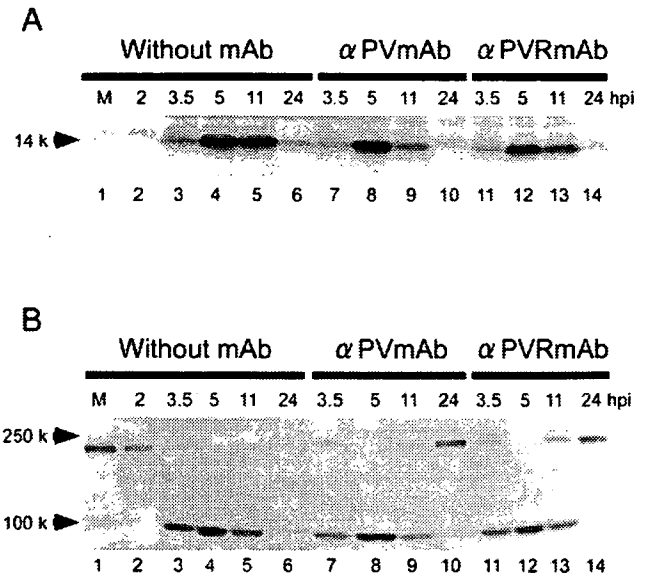

FIG. 6. Western blotting of 2A^{pro} and eIF4G. 2A^{pro} expression (A) or eIF4G cleavage (B) in PV-infected neural cells was detected by Western blot analysis. M (lane 1), mock infection. Neural cells were not treated 2 hpi with MAb (lanes 2 to 6) or were treated 2 hpi with MAb against PV (lanes 7 to 10) or against hPVR (lanes 11 to 14).

any event, a considerable amount of 2A^{pro} still existed 11 hpi even in the presence of MAb.

PV-infected neural cells in the presence of MAb did not exhibit a CPE 11 hpi (Fig. 3B and C), although a significant amount of 2A^{pro} was present in the cells 11 hpi. Another 2A^{pro}-mediated phenomenon, the cleavage of eIF4G, was examined by Western blot analysis with anti-eIF4G antibodies (Fig. 6B). Most eIF4G was cleaved by 3.5 hpi, and no intact eIF4G was detected 5 hpi with or without MAb. In the presence of MAb, intact eIF4G began to appear 11 hpi, when a considerable amount of 2A^{pro} was present (Fig. 6A); only intact eIF4G was detected 24 hpi, whereas, in the absence of MAb, no intact eIF4G was detected 5 hpi or later.

These results indicate that two 2A^{pro}-mediated phenomena, CPE expression and eIF4G cleavage, were suppressed in PV-infected neural cells in the presence of MAb. 2A^{pro}-mediated CPE expression is discussed below. As for eIF4G cleavage, it is possible that 2A^{pro} activity was inhibited by cellular factors or by the compartmentalization of 2A^{pro} from eIF4G in neural cells.

Localization of 2A^{pro}. To determine the localization of 2A^{pro} in neural cells infected with PV, 2A-HA virus was constructed as described in Materials and Methods. The genomic structure of this virus is shown in Fig. 7. The virus had phenotypes similar to those of PV1/Mahoney (data not shown), such as induction of CPE progression in neural cells with or without MAb (Fig. 1), growth profile (Fig. 2), plaque size phenotype, pulse-labeling pattern (Fig. 4A), 2A^{pro} expression (Fig. 6A), and eIF4G cleavage profile (Fig. 6B).

SK-N-SH cells were infected with 2A-HA virus at an MOI of 10, and the localization of 2A^{pro} was investigated 5 and 11 hpi as described in Materials and Methods (Fig. 8). HA-tagged 2A^{pro} was present in the nucleus and cytoplasm 5 hpi with or

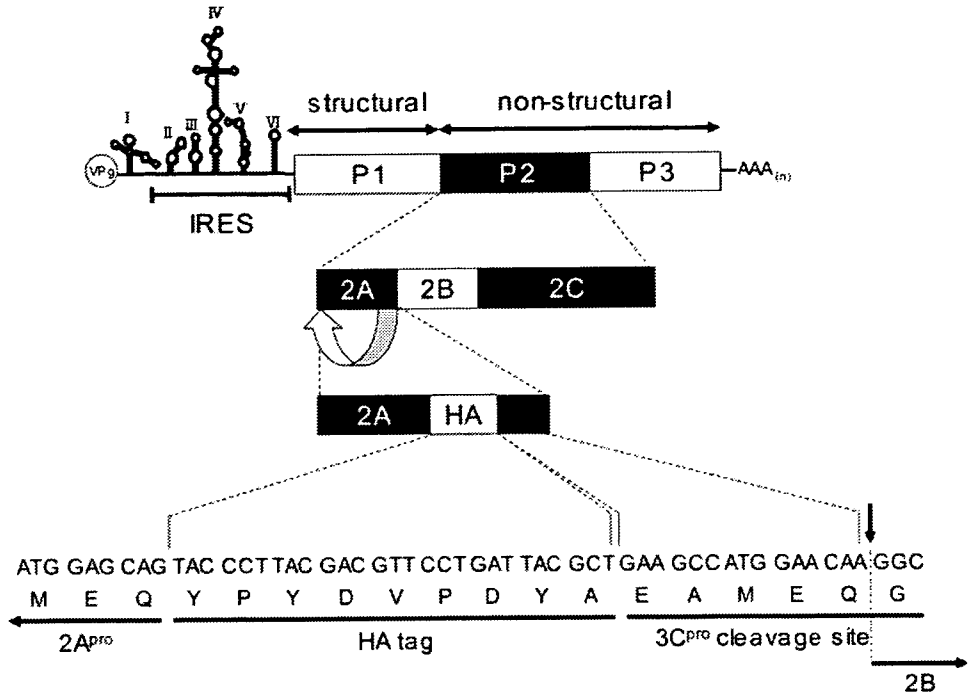

FIG. 7. Structure of the 2A-HA virus genome. VPg represents a viral protein genome located at the 5′ terminus, $AAA_{(n)}$ represents poly(A) located at the 3′ terminus, P1 is a structural (capsid) protein precursor, and P2 and P3 are nonstructural (noncapsid) precursors. Nucleotide and amino acid sequences at the junction between regions 2A and 2B are indicated at the bottom of the figure.

without MAb (Fig. 8A to C). In the presence of MAb, HA-tagged $2A^{pro}$ was detected only in the nucleus 11 hpi (Fig. 8E and F), and the cells did not show signs of the CPE (Fig. 8H and I). In the absence of MAb, however, HA-tagged $2A^{pro}$ was localized both in the nucleus and in the cytoplasm 11 hpi, and the cells displayed typical signs of the CPE by 11 hpi (Fig. 8D and G). These data indicate that $2A^{pro}$ in PV-infected neural cells was imported into the nucleus. Thus, the compartmentation of $2A^{pro}$ from eIF4G in neural cells may result in the appearance of intact eIF4G 11 hpi in the presence of MAb. Similar experiments were carried out with HeLa cells; the results obtained with MAb and without MAb were similar to those obtained for neural cells without MAb (data not shown).

Expression of HA-tagged $2A^{pro}$ alone. To investigate the abilities of $2A^{pro}$ to induce the CPE and to be transported to the nucleus, HA-tagged $2A^{pro}$ alone was expressed in SK-N-SH and HeLa cells by using a mammalian expression vector. The cells were fixed 2 days after transfection and stained as described in Materials and Methods. As shown in Fig. 9, only HeLa cells exhibited the CPE (Fig. 9E), and neural cells appeared not to be damaged (Fig. 9A). HA-tagged $2A^{pro}$ was detected only in the nucleus in neural cells, but it was found both in the nucleus and in the cytoplasm in HeLa cells. HA-tagged $2A^{pro}$ may be synthesized at higher levels in HeLa cells than in SK-N-SH cells. These data indicate that the harmful effect of $2A^{pro}$ observed in HeLa cells is suppressed in neural cells and that HA-tagged $2A^{pro}$ itself has the ability to be distributed to the nucleus.

DISCUSSION

Cultured cells, such as HeLa cells, infected with PV die of a severe CPE. This phenomenon is thought to be attributed mainly to the expression of viral $2A^{pro}$, which is also responsible for eIF4G cleavage and host cell translation shutoff. An exception was reported by Tolskaya et al. (35). Neural cells infected with PV were eventually cured when they were treated with anti-PV hyperimmune serum shortly after infection. This report is a continuation of this observation and indicates the existence of protective mechanisms against PV infection in neural cells.

Since Tolskaya et al. (35) assumed that antibodies penetrate infected cells, we examined the possibility of penetration of MAbs by using HeLa cells and SK-N-SH cells. The results indicated that both cell lines take up MAbs (data not shown). However, it is not likely that MAbs inhibit PV replication inside cells, because the penetration of MAbs into HeLa cells occurred more efficiently than that into SK-N-SH cells (data not shown). Furthermore, the argument by Tolskaya et al. (35) does not correlate with the observation that an anti-hPVR MAb also blocked the PV-induced CPE in neural cells.

Our data strongly suggest that antibody treatment prevents multiple rounds of viral replication and that subsequent rounds of particle propagation inside cells result in CPE expression in neural cells. To confirm this notion, neural cells were infected with defective interfering particles of PV, which were not able to produce progeny virions because of the lack of a capsid protein coding sequence in the genome. Our preliminary results showed that defective interfering particles did not induce

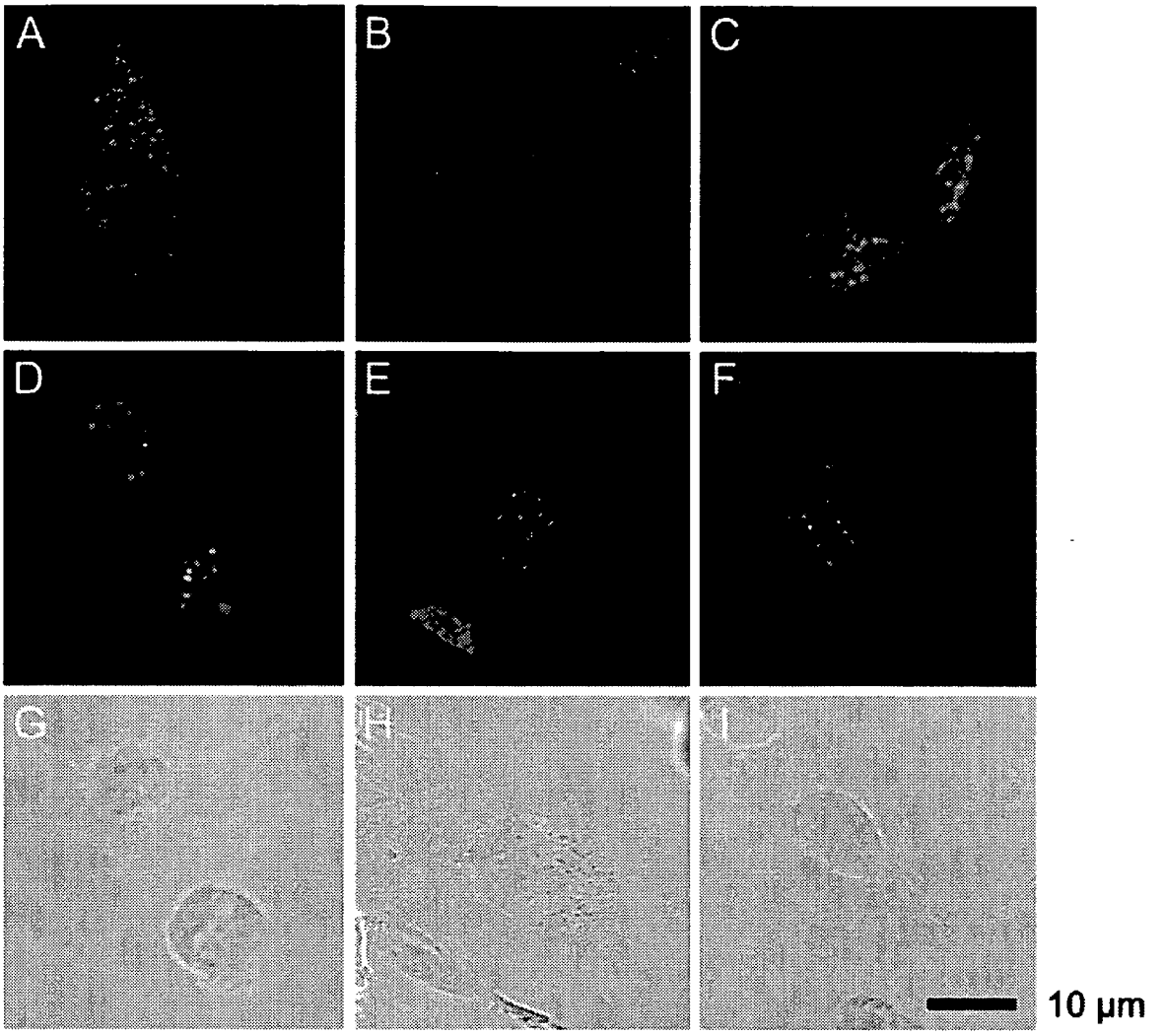

FIG. 8. Localization of HA-tagged $2A^{pro}$ in PV-infected neural cells. Neural cells infected with 2A-HA virus were cultured as described in Materials and Methods. The cells were not treated 2 hpi with MAb (A, D, and G) or were treated 2 hpi with MAb against PV (B, E, and H) or against hPVR (C, F, and I). The cells were fixed 5 hpi (A, B, and C) or 11 hpi (D, E, F, G, H, and I) and subjected to an immunofluorescence study. Red indicates nucleic acids, and green indicates HA-tagged $2A^{pro}$.

a CPE in neural cells but did induce a severe CPE in HeLa cells. However, it is not clear which process in the subsequent infections is necessary to induce the CPE. Indeed, virus yields were not different between infected cell cultures in the presence and in the absence of MAbs. It is known that virus yield is not altered when the efficiency of viral protein synthesis is slightly lowered artificially. This means that PV-specific protein synthesis in infected cells is present in surplus compared with PV-specific RNA synthesis. Thus, CPE expression may depend on the amounts of PV-specific proteins expressed in infected cells. It should be noted that the level of $2A^{pro}$ expression in the absence of MAb was always higher than that in the presence of MAb 11 hpi, when virus production was already complete (Fig. 6A). The expression of $2A^{pro}$ alone in neural cells (Fig. 9) may not be over the threshold needed to induce the CPE under the conditions used in this study. It is also possible that neural and HeLa cells differ in their sensitivities to harmful PV-specific proteins.

PV-specific protein synthesis was inhibited by 7 hpi (Fig. 4A), and virus production was completed by 8 hpi (Fig. 2). Therefore, the amounts of PV antigens were reduced until 24 hpi (Fig. 3). It is possible that PV-specific proteins are degraded by turnover mechanisms in cells. However, the reasons for the rapid disappearance of PV particles are not clear, considering the high stability of PV particles. They may be released into the culture medium. Alternatively, neural cells may possess mechanisms for destroying PV particles.

In the absence of MAb, host cell protein synthesis in infected neural cells continued until at least 9 hpi (data not shown), whereas eIF4G appeared to be completely cleaved by 5 hpi (Fig. 6B). These data suggest the existence of a factor(s) other than eIF4G that compensates for the lack of intact eIF4G in neural cells, although a small amount of residual intact eIF4G may function to continue host cell protein synthesis. It is possible that there are multiple eIF4G-related molecules in neural cells. Molecule p97/NAT1/DAP5 is one

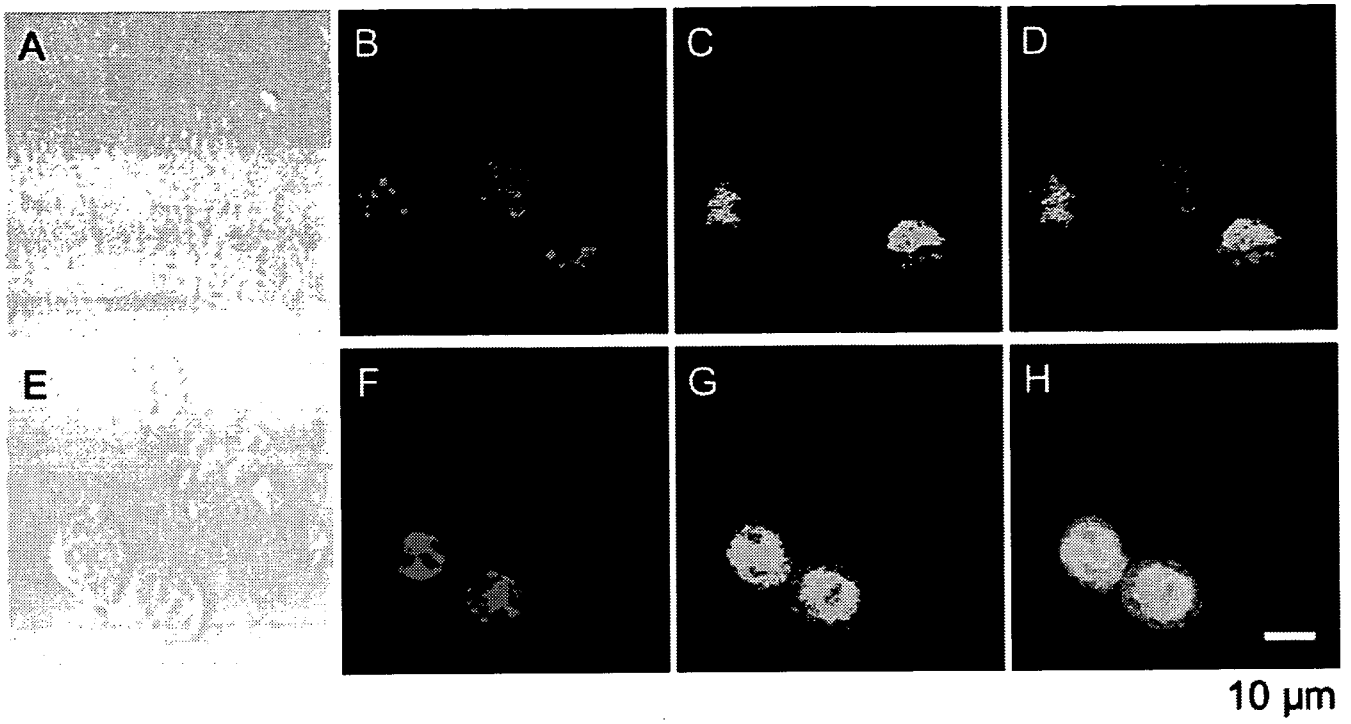

FIG. 9. Transient expression of HA-tagged $2A^{pro}$. Mammalian expression vector pCI-neo encoding HA-tagged $2A^{pro}$ was transfected into cells, which were subjected to an immunofluorescence study. Neural cells (A, B, C, and D) and HeLa cells (E, F, G, and H) were fixed 2 days posttransfection. Red indicates nucleic acids, and green indicates HA-tagged $2A^{pro}$.

example, and it is similar to the C-terminal half of eIF4G (15, 21, 39). Such a factor(s) may be specifically expressed in neural cells and function in place of eIF4G. The factor(s) may be fairly resistant to PV infection, because translation shutoff in neural cells is delayed until 11 hpi.

HA-tagged $2A^{pro}$ is imported into the nucleus. Since the HA tag itself does not show such activity (data not shown), the $2A^{pro}$ moiety of HA-tagged $2A^{pro}$ must carry a region(s) like a nuclear localization signal. Indeed, there are basic amino acid-rich regions in the N-terminal half of $2A^{pro}$. The function(s) of $2A^{pro}$ in the nucleus is not known at present. However, the components of the nuclear pore complex are degraded in PV-infected cells, a process which might disturb nuclear import and export systems and therefore inhibit the cell signaling pathways which induce the onset of an antiviral response (11). According to our preliminary results, the degradation of components of the nuclear pore complex is not due to $2A^{pro}$ (data not shown). In addition, our data suggest that $2A^{pro}$ imported into the nucleus of neural cells is silent in the induction of host translation shutoff and CPE progression. Thus, $2A^{pro}$ may be active only in the cytoplasm. Furthermore, it was reported that $2A^{pro}$ may be involved in PV replication through mechanisms independent of its protease activity (22, 27, 40).

Besides $2A^{pro}$, 2BC is cytotoxic in HeLa cells, although its cytotoxicity is lower than that of $2A^{pro}$ (1, 2). Since the PV-infected neural cells used in this study did not show a CPE when MAb to PV or the hPVR was added to the culture 2 hpi, it is possible that the MAb inhibits the cytotoxicity of 2BC in neural cells. Alternatively, 2BC may not have any toxic effect on neural cells.

The mechanism responsible for the inhibition of PV IRES activity in neural cells is unknown at present. Upon PV infection, neural cells may respond by producing a factor(s) that inhibits PV IRES activity. A search for such a factor(s) is essential to understanding the neurovirulence of PV and is presently being conducted. Such a putative factor(s) may be useful as an anti-PV agent.

Our hypothesis is summarized in Fig. 10. In the presence of MAb against PV or the hPVR, multiple rounds of viral replication are blocked. Thus, the viral infection cycle induced by the primary infection can be observed. As shown in Fig. 2, viral replication in neural cells is not affected by the addition of MAb 2 hpi. eIF4G is then cleaved by $2A^{pro}$ in the cytoplasm by 5 hpi. Host translation continues without detectable intact eIF4G, probably because a neural cell factor(s) compensates for its absence. By 7 hpi, PV-specific protein synthesis ceases due to unknown mechanisms that may involve the induction of a factor(s) to prevent PV IRES activity. This effect results in inhibition of the accumulation of PV-specific proteins. Existing $2A^{pro}$ in neural cells is imported into the nucleus by 11 hpi, and intact eIF4G begins to appear because of $2A^{pro}$ localization in the nucleus. The resurrection of intact eIF4G supports host translation. As a result, PV-infected neural cells do not show a CPE and are eventually cured of PV infection.

Neural cells in the central nervous system (CNS) may possess a specific immune system response that differs from that of other tissues. It should be noted that the curing of PV-infected neural cells in the CNS of monkeys has been suggested (6). Microglia derived from monocytes are mainly responsible for immune system activity in the CNS. Besides the utilization of

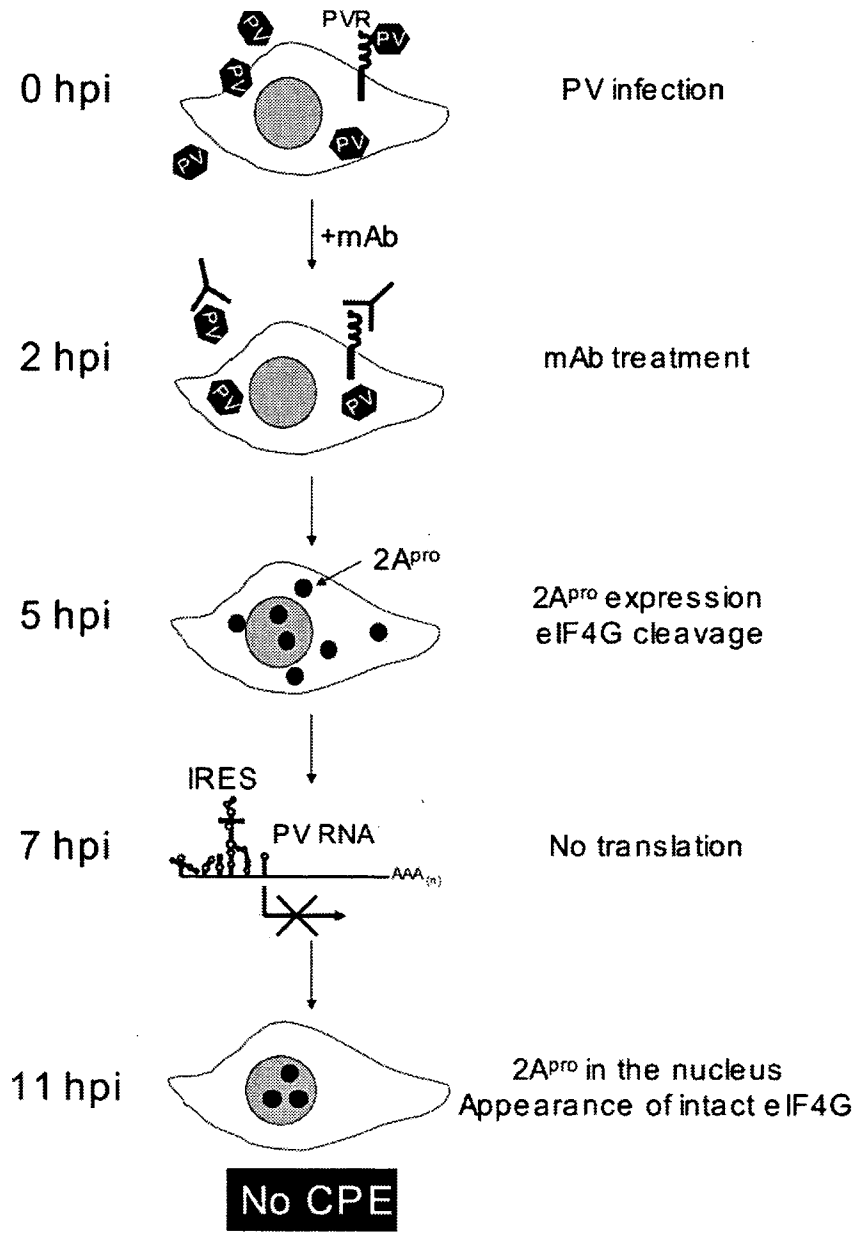

FIG. 10. Schematic explanation of the process responsible for inhibition of the PV-induced CPE in neural cells by MAb against PV or against hPVR. See the legend to Fig. 7 for definitions of abbreviations.

microglia, it is possible that neural cells themselves prepare specific intracellular immune system features, such as double-stranded RNA-dependent protein kinase and RNA interference. The protective response against PV infection reported here may be an intracellular immune system response specific to neural cells. Alternatively, this kind of intracellular immune system may also be present in HeLa cells but may be masked. Much work should be done to elucidate the mechanisms of the protective response observed only in neuroblastoma cells.

ACKNOWLEDGMENTS

We thank Etsuko Suzuki and Yuri Matsushita for help in preparing the manuscript.

This work was supported by a Grant-in-Aid for Specially Promoted Research from the Ministry of Education, Culture, Sports, Science, and Technology of Japan.

REFERENCES

1. **Aldabe, R., A. Barco, and L. Carrasco.** 1996. Membrane permeabilization by poliovirus proteins 2B and 2BC. J. Biol. Chem. **271**:23134–23137.
2. **Aldabe, R., A. Irurzun, and L. Carrasco.** 1997. Poliovirus protein 2BC increases cytosolic free calcium concentrations. J. Virol. **71**:6214–6217.
3. **Barco, A., E. Feduchi, and L. Carrasco.** 2000. A stable HeLa cell line that inducibly expresses poliovirus $2A^{pro}$: effects on cellular and viral gene expression. J. Virol. **74**:2383–2392.
4. **Belsham, G. J., and N. Sonenberg.** 1996. RNA-protein interactions in regulation of picornavirus RNA translation. Microbiol. Rev. **60**:499–511.
5. **Bienz, K., D. Egger., Y. Rasser., and W. Bossart.** 1980. Kinetics and location of poliovirus macromolecular synthesis in correlation to virus-induced cytopathology. Virology **100**:390–399.

6. **Bodian, D.** 1949. Histopathlogic basis of clinical finding in poliomyelitis. Am. J. Med. **6**:563–578.
7. **Dales, S., H. J. Eggers., I. Tam., and G. E. Palade.** 1965. Electron microscopic study of the formation of poliovirus. Virology 379–389.
8. **Ehrenfeld, E.** 1996. Initiation of translation by picornavirus RNAs, p. 549–573. *In* J. W. B. Hershey, M. B. Mathews, and N. Sonenberg (ed.), Translational control. Cold Spring Harbor Laboratory Press, Cold Spring Harbor, N.Y.
9. **Ehrenfeld, E.** 1982. Poliovirus-induced inhibition of host-cell protein synthesis. Cell **28**:435–436.
10. **Etchison, D., S. C. Milburn, I. Edery, N. Sonenberg, and J. W. Hershey.** 1982. Inhibition of HeLa cell protein synthesis following poliovirus infection correlates with the proteolysis of a 220,000-dalton polypeptide associated with eucaryotic initiation factor 3 and a cap binding protein complex. J. Biol. Chem. **257**:14806–14810.
11. **Gustin, K. E., and P. Sarnow.** 2001. Effects of poliovirus infection on nucleocytoplasmic trafficking and nuclear pore complex composition. EMBO J. **20**:240–249.
12. **Hambidge, S. J., and P. Sarnow.** 1992. Translational enhancement of the poliovirus 59 noncoding region mediated by virus-encoded polypeptide 2A. Proc. Natl. Acad. Sci. USA **89**:10272–10276.
13. **Hanecak, R., B. L. Semler, C. W. Anderson, and E. Wimmer.** 1982. Proteolytic processing of poliovirus polypeptides: antibodies to polypeptide P3-7c inhibit cleavage at glutamine-glycine pairs. Proc. Natl. Acad. Sci. USA **79**: 3973–3977.
14. **Holland, J. J.** 1962. Irreversible eclipse of poliovirus by HeLa cells. Virology **16**:163–176.
15. **Imataka, H., H. S. Olsen, and N. Sonenberg.** 1997. A new translational regulator with homology to eukaryotic translation initiation factor 4G. EMBO J. **16**:817–825.
16. **Krausslich, H. G., M. J. Nicklin, H. Toyoda, D. Etchison, and E. Wimmer.** 1987. Poliovirus proteinase 2A induces cleavage of eucaryotic initiation factor 4F polypeptide p220. J. Virol. **61**:2711–2718.
17. **Krausslich, H. G., and E. Wimmer.** 1988. Viral proteinases. Annu. Rev. Biochem. **57**:701–754.
18. **Lamphear, B. J., R. Kirchweger., T. Skern., and R. E. Rhoads.** 1995. Mapping of functional domains in eukaryotic protein synthesis initiation factor 4G (eIF4G) with picornaviral proteases-implications for cap-dependent and cap-independent translational initiation. J. Biol. Chem. **270**:21975–21983.
19. **Lee, C. K., and E. Wimmer.** 1988. Proteolytic processing of poliovirus polyprotein: elimination of 2Apro-mediated, alternative cleavage of polypeptide 3CD by in vitro mutagenesis. Virology **166**:405–414.
20. **Leibowitz, R., and S. Penman.** 1971. Regulation of protein synthesis in HeLa cells. 3. Inhibition during poliovirus infection. J. Virol. **8**:661–668.
21. **Levy-Strumpf, N., L. P. Deiss, H. Berissi, and A. Kimchi.** 1997. DAP-5, a novel homolog of eukaryotic translation initiation factor 4G isolated as a putative modulator of gamma interferon-induced programmed cell death. Mol. Cell. Biol. **17**:1615–1625.
22. **Lu, H. H., X. Y. Li, A. Cuconati, and E. Wimmer.** 1995. Analysis of picornavirus $2A^{pro}$ proteins: separation of proteinase from translation and replication functions. J. Virol. **69**:7445–7452.
23. **McBride, A. E., A. Schlegel, and K. Kirkegaard.** 1996. Human protein Sam68 relocalization and interaction with poliovirus RNA polymerase in infected cells. Proc. Natl. Acad. Sci. USA **93**:2296–2301.
24. **Meerovitch, K., J. Pelletier, and N. Sonenberg.** 1989. A cellular protein that binds to the 5′-noncoding region of poliovirus RNA: implications for internal translation initiation. Genes Dev. **3**:1026–1034.
25. **Meerovitch, K., Y. V. Svitkin, H. S. Lee, F. Lejbkowicz, D. J. Kenan, E. K. Chan, V. I. Agol, J. D. Keene, and N. Sonenberg.** 1993. La autoantigen enhances and corrects aberrant translation of poliovirus RNA in reticulocyte lysate. J. Virol. **67**:3798–3807.
26. **Merrick, W. C., and J. W. B. Hershey.** 1996. The pathway and mechanism of eukaryotic protein synthesis, p. 31–69. Cold Spring Harbor Laboratory Press, Cold Spring Harbor, N.Y.
27. **Molla, A., A. V. Paul., M. Schmid., S. K. Jang., and E. Wimmer.** 1993. Studies on dicistronic polioviruses implicate viral proteinase 2Apro in RNA replication. Virology **196**:739–747.
28. **Pallansch, M. A., O. M. Kew, B. L. Semler, D. R. Omilianowski, C. W. Anderson, E. Wimmer, and R. R. Rueckert.** 1984. Protein processing map of poliovirus. J. Virol. **49**:873–880.
29. **Pelletier, J., and N. Sonenberg.** 1988. Internal initiation of translation of eukaryotic mRNA directed by a sequence derived from poliovirus RNA. Nature **334**:320–325.
30. **Sachs, A. B., P. Sarnow., and M. W. Hentze.** 1997. Starting at the beginning, middle, and end: translation initiation in eukaryotes. Cell **89**:831–838.
31. **Shiroki, K., T. Ishii, T. Aoki, M. Kobashi, S. Ohka, and A. Nomoto.** 1995. A new *cis*-acting element for RNA replication within the 5′ noncoding region of poliovirus type 1 RNA. J. Virol. **69**:6825–6832.
32. **Shiroki, K., T. Isoyama, S. Kuge, T. Ishii, S. Ohmi, S. Hata, K. Suzuki, Y. Takasaki, and A. Nomoto.** 1999. Intracellular redistribution of truncated La protein produced by poliovirus $3C^{pro}$-mediated cleavage. J. Virol. **73**:2193–2200.
33. **Skern, T., and H. D. Liebig.** 1994. Picornains 2A and 3C. Methods Enzymol. **244**:583–595.
34. **Sonenberg, N.** 1990. Poliovirus translation. Curr. Top. Microbiol. Immunol. **161**:23–47.
35. **Tolskaya, E. A., T. A. Ivannikova, M. S. Kolesnikova, S. G. Drozdov, and V. I. Agol.** 1992. Postinfection treatment with antiviral serum results in survival of neural cells productively infected with virulent poliovirus. J. Virol. **66**:5152–5156.
36. **Toyoda, H., M. J. Nicklin, M. G. Murray, C. W. Anderson, J. J. Dunn, F. W. Studier, and E. Wimmer.** 1986. A second virus-encoded proteinase involved in proteolytic processing of poliovirus polyprotein. Cell **45**:761–770.
37. **Waggoner, S., and P. Sarnow.** 1998. Viral ribonucleoprotein complex formation and nucleolar-cytoplasmic relocalization of nucleolin in poliovirus-infected cells. J. Virol. **72**:6699–6709.
38. **Wimmer, E., C. U. Hellen, and X. Cao.** 1993. Genetics of poliovirus. Annu. Rev. Genet. **27**:353–436.
39. **Yamanaka, S., K. S. Poksay, K. S. Arnold, and T. L. Innerarity.** 1997. A novel translational repressor mRNA is edited extensively in livers containing tumors caused by the transgene expression of the apoB mRNA-editing enzyme. Genes Dev. **11**:321–333.
40. **Yu, S. F., P. Benton, M. Bovee, J. Sessions, and R. E. Lloyd.** 1995. Defective RNA replication by poliovirus mutants deficient in 2A protease cleavage activity. J. Virol. **69**:247–252.
41. **Ziegler, E., A. M. Borman., F. G. Deliat., H. D. Liebig., D. Jugovic., K. M. Kean., T. Skern., and E. Kuechler.** 1995. Picornavirus 2A proteinase-mediated stimulation of internal initiation of translation is dependent on enzymatic activity and the cleavage products of cellular proteins. Virology **213**: 549–557.

RESEARCH LETTER

Increase of Disease Duration of Amyotrophic Lateral Sclerosis in a Mouse Model by Transgenic Small Interfering RNA

Many lines of evidence show that mutant *SOD1* in familial amyotrophic lateral sclerosis (ALS) gains a novel toxic property, causing neuronal cell death.[1] A simple and attractive therapeutic approach, therefore, is to inhibit the expression of mutant *SOD1*. Small interfering RNA (siRNA) can strongly suppress expression of the target gene and become a powerful tool in gene therapy for dominantly inherited neurodegenerative diseases.[2] Recently, we reported that the onset of ALS symptoms was extremely delayed in $SOD1^{G93A}$ transgenic (Tg) mice when crossed with the Tg mouse overexpressing siRNA to *SOD1*.[3] Here, we furthermore found that this transgenic siRNA could markedly slow the progression of the disease as well.

Methods. We designed the siRNA (GGUGGAAUGAAGAAAGUAC of the sense sequence) as a good and common target region of siRNA to human and mouse *SOD1* messenger RNA.[4] By overexpressing this siRNA with mismatch mutations, we developed the anti-*SOD1* siRNA Tg mouse as previously reported.[3] Briefly, an anti-*SOD1* short hairpin RNA (shRNA) construct was made using human U6 promoter and UUCAAGAGA as a loop sequence. This shRNA expression vector was introduced to mouse ES cells, and the selected ES clone with an approximately 80% reduced level of endogenous *SOD1* was injected into C57BL/6 blastocysts. The resulting chimeric male mouse was mated with C57BL/6, and germline transmission of the shRNA was confirmed. Furthermore, this anti-*SOD1* siRNA Tg mouse was mated with $SOD1^{G93A}$ Tg mice (G1H line from Jackson Laboratories Bar Harbor, Me, backcrossed to C57BL/6 mice) to generate the double Tg mice.

Protein samples were extracted from whole spinal cords; the medial one third of the frontal cortex, including motor cortex; and other areas of cerebral cortex from 3 double Tg mice and 3 $SOD1^{G93A}$ Tg mice. The samples were homogenized in buffer containing 0.1% sodium dodecyl sulfate (SDS), 1% Triton X-100, 1% sodium deoxycholate, and 1mM phenylmethanesulfonyl fluoride. Equal amounts of extracted protein were mixed with Laemmli sample buffer (BioRad, Hercules, Calif), denatured, and separated on 15% SDS polyacrylamide gel electrophoresis. Following transfer onto a polyvinylidene fluoride membrane (BioRad), blots were probed with anti-*SOD1* polyclonal antibody S-100 (Stressgen Biotechnologies, San Diego, Calif). The amount of *SOD1* protein level was estimated by band signal intensity with standard recombinant human *SOD1* (Wako, Tokyo, Japan).

For measuring enzymatic activity, a half of whole brain was homogenized in 5-volume (weight-volume ratio) homogenizing buffer (0.25 M sucrose; 10 mM Tris-hydrochloric acid, pH 7.4; 1 mM ethylenediaminetetraacetic acid). The homogenate was centrifuged at 78 000 g for 60 minutes and the supernatant was removed and saved. Copper-zinc superoxide dismutase activity was measured according to the manufacturer's instruction (SOD Assay Kit–WST; Dojindo Molecular Technologies, Inc, Tokyo).

For immunohistochemical analysis, the lumbar segments of the spinal cords were removed and fixed in 4% paraformaldehyde in phosphate-buffered saline (pH 7.4). The sections (10-μm thick) of the spinal cord at the level of the third lumbar (L3) vertebra were incubated with anti-*SOD1* polyclonal antibody S-100 (1:1000 to 1:15 000, Stressgen Biotechnologies). Staining was visualized by diaminobenzidine.

Results. The crossed double Tg mice had much reduced expression of mutant *SOD1* protein in the multiple areas of the nervous system compared with that in $SOD1^{G93A}$ Tg littermates; the mean±SD *SOD1* protein contents of frontal cortex, including motor cortex; the other area of cerebral cortex; and spinal cord in $SOD1^{G93A}$ Tg mice and double Tg mice were 2.48±0.36, 2.75±0.15, and 3.63±0.26 and 0.84±0.16, 1.03±0.20, and 1.44±0.34 mg per gram of tissue (mean reduction rate, 66.0%, 62.4%, and 69.8%, respectively). The mean±SD enzymatic activity of *SOD1* in $SOD1^{G93A}$ Tg mice and double Tg mice brain was 527.0±22.8 and 172.3±36.3 U/mg, respectively (mean reduction rate, 67.3%). On immunohistochemical analysis, there was no remarkable difference in the *SOD1* immunoreactivity of motor and sensory neurons in the spinal cord of double Tg mice (data not shown).

The double Tg mice showed ALS symptoms after about 10 months old. The symptoms of the double Tg mice were almost same as those of $SOD1^{G93A}$ Tg mice (hind-limb paresis and muscle atrophy, lack of mobility followed by breathing difficulties) except for lack of tremor. Onset of motor function loss was observed at a mean±SD age of 358.6±41.0 days (range, 302-520 days) in the double Tg mice (n=5) and 127.3±1.2 days (range, 115-135 days) in $SOD1^{G93A}$ Tg mice (n=23) (difference, $P=.003$ by log-rank test). The mean±SD survival time was also much prolonged in the double Tg mice (395.2±45.3 days; range, 326-574 days) compared with that in $SOD1^{G93A}$ Tg mice (145.9±1.7 days; range, 130-157 days) (difference, $P=.003$). Most importantly, the disease progression of

limb weakness was markedly slowed and the duration from onset of the hind-limb dysfunction to death was significantly prolonged in the double Tg mice compared with that in the $SOD1^{G93A}$ Tg mice (double Tg mice, 36.6±5.7 days; $SOD1^{G93A}$ Tg mice, 18.6±1.6 days; $P=.02$).

Comment. In the previous reports in which siRNA-expressing lentivirus[5] or adeno-associated[6] virus was injected to muscles of $SOD1^{G93A}$ Tg mice, the onset of weakness was markedly delayed,[5,6] but disease progression did not significantly change.[5] In another report[7] in which siRNA-expressing lentivirus was injected to lumbar spinal cord of $SOD1^{G93A}$ Tg mice, the onset and progression of the hind-limb dysfunction were delayed, but the disease duration was not described. In these reports, siRNA did not reach all motoneuron innervating bulbar and respiratory muscles of which paresis should influence the life span of this ALS mouse model. In contrast, all motoneurons and glial cells throughout the central nervous system in our crossed double Tg mice had siRNA expressed by the shRNA transgene. Therefore, our study is considered to be better than the other 3 reports in evaluating the siRNA effect on the disease duration after the onset until death. We clearly proved that siRNA-mediated gene silencing can slow the disease progression and increase the disease duration of ALS in a mouse model, suggesting that treatment with siRNA after the onset of disease is beneficial for slowing down the progression and expanding the life span of patients with this fatal disease.

Takanori Yokota, MD, PhD
Hiroki Sasaguri, MD
Yuki Saito, MD, PhD
Hiromi Yamada
Toshinori Unno
Yuki Yamamoto
Takayuki Kubodera, MD, PhD
Masayuki Anzai, PhD
Tasuku Mitani, PhD
Hidehiro Mizusawa, MD, PhD

Correspondence: Dr Yokota, Department of Neurology and Neurological Science, Tokyo Medical and Dental University, 1-5-45 Yushima Bunkyo-ku, Tokyo 113-8519, Japan (tak-yokota.nuro@tmd.ac.jp).

Author Contributions: *Study concept and design:* Yokota. *Acquisition of data:* Yokota, Sasaguri, Saito, Yamada, Unno, Yamamoto, Kubodera, Anzai, and Mitani. *Analysis and interpretation of data:* Yokota. *Drafting of the manuscript:* Yokota and Mitani. *Critical revision of the manuscript for important intellectual content:* Yokota, Sasaguri, Saito, Yamada, Unno, Yamamoto, Kubodera, Anzai, and Mitani. *Statistical analysis:* Yokota. *Obtained funding:* Yokota, Sasaguri, Saito, Yamada, Unno, Yamamoto, Kubodera, Anzai, and Mitani. *Administrative, technical, and material support:* Yokota. *Study supervision:* Yokota and Mizusawa.
Financial Disclosure: None reported.
Funding/Support: This study was supported by grants from the Ministry of Education, Science, and Culture; the Ministry of Health, Labor, and Welfare; the Nakabayashi Trust for Amyotrophic Lateral Sclerosis Research; and the Kato Memorial Bioscience Foundation.

1. Cleveland DW. From Charcot to SOD1: mechanisms of selective motor neuron death in ALS. *Neuron.* 1999;24:515-520.
2. Davidson BL, Paulson HL. Molecular medicine for the brain: silencing of disease genes with RNA interference. *Lancet Neurol.* 2004;3:145-149.
3. Saito Y, Yokota T, Mitani T, et al. Transgenic small interfering RNA halts amyotrophic lateral sclerosis in a mouse model. *J Biol Chem.* 2005;280:42826-42830.
4. Yokota T, Miyagishi M, Hino T, et al. siRNA-based inhibition specific for mutant SOD1 with single nucleotide alternation in familial ALS, compared with ribozyme and DNA enzyme. *Biochem Biophys Res Commun.* 2004;314:283-291.
5. Ralph GS, Radcliffe PA, Day DM, et al. Silencing mutant SOD1 using RNAi protects against neurodegeneration and extends survival in an ALS model. *Nat Med.* 2005;11:429-433.
6. Miller TM, Kaspar BK, Kops GJ, et al. Virus-delivered small RNA silencing sustains strength in amyotrophic lateral sclerosis. *Ann Neurol.* 2005;57:773-776.
7. Raoul C, Abbas-Terki T, Bensadoun JC, et al. Lentiviral-mediated silencing of SOD1 through RNA interference retards disease onset and progression in a mouse model of ALS. *Nat Med.* 2005;11:423-428.

Guidelines for Letters

Letters discussing a recent *Archives of Neurology* article will have the best chance of acceptance if they are received within 4 weeks of the article's publication date. They should not exceed 400 words of text and 5 references. Letters reporting original research should not exceed 600 words and 6 references. All letters should include a word count. Letters must not duplicate other material published or submitted for publication. Letters will be published at the discretion of the editors and are subject to editing and abridgment. A signed statement for authorship criteria and responsibility, financial disclosure, copyright transfer, and acknowledgment is required for publication. Letters not meeting these specifications are generally not considered. Before submitting a Research Letter, please review the Instructions for Authors (September 2004 or http://archneur.ama-assn.org/misc/ifora.dtl).

Available online at www.sciencedirect.com
SCIENCE DIRECT
ELSEVIER
Biochemical and Biophysical Research Communications 340 (2006) 263–267
BBRC
www.elsevier.com/locate/ybbrc

In vivo delivery of small interfering RNA targeting brain capillary endothelial cells

Taro Hino [a,1], Takanori Yokota [a,*], Shingo Ito [b], Kazutaka Nishina [a], Young-Sook Kang [b,c], Shinobu Mori [b], Satoko Hori [b], Takashi Kanda [a], Tetsuya Terasaki [b], Hidehiro Mizusawa [a,1]

[a] *Department of Neurology and Neurological Science, Graduate School, Tokyo Medical and Dental University, Tokyo, Japan*
[b] *Department of Molecular Biopharmacy and Genetics, Graduate School of Pharmaceutical Sciences, Tohoku University, Sendai, Japan*
[c] *College of Pharmacy, Sookmyung Women's University, Seoul, Republic of Korea*

Received 24 November 2005
Available online 9 December 2005

Abstract

Brain capillary endothelial cells (BCECs) play an important role in blood–brain barrier (BBB) functions and pathophysiologic mechanisms in brain ischemia and inflammation. We try to suppress gene expression in BCECs by intravenous application of small interfering RNA (siRNA). After injection of large dose siRNA with hydrodynamic technique to mouse, suppression of endogenous protein and the BBB function of BCECs was investigated. The brain-to-blood transport function of organic anion transporter 3 (OAT3) that expressed in BCECs was evaluated by Brain Efflux Index method in mouse. The siRNA could be delivered to BCECs and efficiently inhibited endogenously expressed protein of BCECs. The suppression effect of siRNA to OAT3 is enough to reduce the brain-to-blood transport of OAT3 substrate, benzylpenicillin at BBB. The in vivo siRNA-silencing method with hydrodynamic technique may be useful for the study of BBB function and gene therapy targeting BCECs.

Keywords: Small interfering RNA; Blood–brain barrier; Organic anion transporter 3; Brain ischemia; Brain inflammation; Drug delivery system

In brain ischemia and inflammation, the brain capillary endothelial cells (BCECs) have no longer been regarded as an inert vascular lining that is injured and morphologically changed, but actively play many important roles of these pathophysiologic mechanisms. The inhibition of signaling molecule in BCECs of vascular endothelial growth factor (VEGF)-induced vasogenic edema can reduce an ischemic lesion [1]. The inflammatory cell adhesion molecules expressed in BCECs induced by ischemia, such as intercellular adhesion molecule (ICAM) and E-selectin, can be a target molecule [2,3] for the therapy of these diseases. Because leukocytes activation and adhesion to BCECs are believed to contribute to additional, secondary neuronal injury after reperfusion [4] and initiate immune-mediated encephalopathy such as multiple sclerosis [5]. Endothelial nitric oxide synthases expressed in BCECs are also a possible target molecule. In cerebral ischemia, nitric oxide is increased and works as a prooxidant via peroxynitrite [6]. Therefore, BCECs are an important platform in the cerebral ischemia and inflammation, and express many constitutively or transiently expressed molecules which might be a therapeutic target for these pathologies.

RNA interference is a powerful tool for post-transcriptional gene silencing. Recently, we showed an in vitro model whose function of the transporter protein expressed in BCECs is inhibited by siRNA [7]. Here, we try to introduce siRNA by hydrodynamic, intravenous injection method from mouse tail vein and investigate the siRNA effect on brain-to-blood transport function by inhibiting organic anion transporter 3 (OAT3) with Brain Efflux Index method.

* Corresponding author. Fax: +81 3 5803 0169.
E-mail address: tak-yokota.nuro@tmd.ac.jp (T. Yokota).
[1] 21st century COE Program on Brain Integration and it's Disorders.

0006-291X/$ - see front matter © 2005 Elsevier Inc. All rights reserved.
doi:10.1016/j.bbrc.2005.11.173

Materials and methods

Effect of siRNA on expression of recombinant OAT3 in culture cells. The mOAT3cDNA was subcloned from pGEM-HEN/Roct (OAT3) [8] into the *Renilla* luciferase expression vector, psiCHECK-1 (Promega).

Human embryonic kidney 293 (HEK293) cells were transfected with 80 ng of *Renilla* luciferase-fused OAT3 expression vector, 20 ng of *firefly* luciferase expression vector (pGL3; Promega), and 25 nM siRNA in each well of 24-well plates. *Renilla* luciferase activity was normalized with *firefly* luciferase activity. The luciferase activities were analyzed after 24 h after transfection using the Dual Luciferase System (Promega).

Effect of siRNA on uptake of OAT3 substrate in culture cells. The mOAT3 cDNA was subcloned into the pcDNA3 vector. HEK293 cells in 6-well plates were transfected by 0.5 μg of pcDNA3/OAT3 or vector alone with 100 nM siRNA using the Lipofectamine 2000 (Invitrogen). Twenty-four hours after transfection, the cells were passaged into the 24-well plates, and after another 24 h the cells were washed with phosphate-buffered saline (PBS). The uptake study was initiated at 37 °C by applying 200 μl PBS containing 0.5 μCi [^{3}H]benzylpenicillin to estimate the volume of adherent water. After incubation for 2 min, the radioactivities of ^{3}H in the cells were measured. The uptake of [^{3}H]benzylpenicillin was expressed as the ratio to control siRNA (shuffle sequence).

Animals. Adult male of Institute of Cancer Research (ICR) mice, weighing 35–42 g and age 9–10 weeks, were purchased from Charles River Laboratories. All experiments were approved by the Animal Experiment Committee of Tokyo Medical and Dental University.

In vivo transduction of siRNA with hydrodynamic injection method. Hydrodynamic injection method has been performed according to a previously reported method in mice [9]. The 50 μg siRNA in a volume equivalent to 5–10% of the body weight was rapidly injected in 3–5 s into the mouse tail vein. For comparison, the same amount of siRNA in 0.2 ml PBS was injected slowly in more than 60 s into the mouse tail vein as a regular intravenous injection method.

Brain small vascular fractionation and Western blot analysis. Mice brains were harvested 24 h after application of 50 μg siRNA SOD1 with the hydrodynamic or regular injection method. The total brain homogenate [10] and the brain vascular fraction of small vessels were prepared using a modified method reported previously [11]. Briefly, brains were homogenized in Dulbecco's modified Eagle's medium (DMEM). The homogenates were dissociated further with 0.005% (wt/vol) dispase (grade 1; Roche Diagnostic) at 37 °C for 2 h. After centrifugation (800*g*, 5 min), the pellets were suspended with a dextran solution (M_w 70,000; 15% wt/vol; Sigma) and centrifuged (4 °C, 4500*g* for 10 min). The pellets were resuspended with 0.05 M PBS for 10 min. After centrifugation (800*g*, 5 min), the final pellets of small vessels were resuspended in lysis buffer (20 mM Tris–HCl, 0.1% SDS, and 1% Triton).

Fractionated mouse brain tissues and mouse brain capillary endothelial cell line [12] cells were homogenized in buffer containing 10 mM Tris–HCl (pH 7.4), 1 mM EDTA, 150 mM NaCl, 4% Chaps, 1 mM phenylmethylsulfonyl fluoride (PMSF), and a protease-inhibitor cocktail (Complete-Mini; Roche Diagnostic). The 2.5 μg samples were separated with 7.5% SDS–polyacrylamide mini-gel (Bio-Rad) and transferred to a polyvinylidene difluoride membrane. The membrane was probed with anti-glucose-transporter-1 antibodies (Alpha Diagnostic International) or anti-SOD1 antibodies (Stressgen Biotechnologies) and visualized by using an ECL Western blot system (Amersham–Pharmacia).

Assay for efflux function of OAT3 in vivo. Fifty micrograms of siRNA OAT3 or control siRNA was delivered to brain capillary endothelial cells with hydrodynamic injection via the tail vein. After 36 h, the in vivo brain efflux experiments were carried out using Brain Efflux Index (BEI) method as described previously [13]. Each mouse was anesthetized intramuscularly with a mixture of ketamine (125 mg/kg) and xylazine (1.22 mg/kg), then mounted on a stereotaxic frame (SRS-6; Narishige), to hold the head in position. Using a dental drill, a bore hole was made 3.8 mm lateral to the bregma. Then, extracellular fluid buffer (122 mM NaCl, 25 mM $NaHCO_3$, 3 mM KCl, 1.4 mM $CaCl_2$, 1.2 mM $MgSO_4$, 0.4 mM K_2HPO_4, 10 mM D-glucose, and 10 mM Hepes, pH 7.4) containing 96 nCi [^{3}H]benzylpenicillin and 4.8 nCi [^{14}C]inulin was injected over a period 1 min using a 5.0-μl microsyringe (Hamilton Reno) fitted with a fine needle at a depth of 2.5 mm from the surface of the scalp, i.e., the secondary somatosensory cortex 2 (S2) region. The needle was left in this configuration for an additional 4 min to prevent reflux of the injected solution along the injection track, before being slowly retracted. After 40 min, the whole brain was subsequently removed and the left cerebrum was isolated. After weighing each of these, tissue samples were solubilized in 2 N NaOH at 60 °C for 1 h and then mixed with Hionic-fluor (Packard). The radioactivity in each sample was assayed in a liquid scintillation counter equipped with an appropriate crossover correction for ^{3}H and ^{14}C (LS-6500; Beckman).

The BEI was defined by Eq. (1) and the percentage of substrate remaining in the ipsilateral cerebrum was determined from Eq. (2).

$$\mathrm{BEI}(\%) = \frac{\text{test substrate undergoing efflux at the BBB}}{\text{test substrate injected into the brain}} \times 100 \quad (1)$$

$$\text{100-BEI}(\%) = \frac{(\text{amount of test substrate in the brain/amount of reference in the brain})}{(\text{concentration of test substrate injected/concentration of reference injected})} \times 100. \quad (2)$$

The percentage of [^{3}H]benzylpenicillin remaining in the brain is given by (100-BEI).

The data were used when the remaining amount of [^{14}C]inulin in the brain was more than 15% of the injected amount. No significant difference was observed in the remaining percentage of [^{14}C]inulin, which is a non-permeable marker, among all samples (#1, 39.7 ± 3.5%; #2, 27.5 ± 3.4%; #3, 31.4 ± 2.9%; #2 shuffle, 28.9 ± 2.2%) (ANOVA), showing that the hydrodynamic injection of siRNA did not damage the integrity of BBB.

Data analysis. All data represent means ± SEM. An unpaired, two-tailed Student's *t* test was used to determine the significance of differences between two group means. (The difference is certified when $P < 0.05$.)

Results

siRNA directed against the OAT3 and SOD1 genes

Sense sequences of the siRNA designed to OAT3 and SOD1 genes are described as follows. The siRNA of shuffle sequence of siRNA OAT3 #2 and siRNA against unrelated gene, GBV-B virus, were used as negative controls. Uppercase letters at 3′ end indicate deoxyribonucleotides.

siRNA OAT3 #1:	5′-ucuacaacagcaccagagaTT-3′
siRNA OAT3 #2:	5′-ccauuaucuugaauguggaTT-3′
siRNA OAT3 #3:	5′-aaacaaagcaggagccagaTT-3′
siRNA-shuffle sequence:	5′-agugguaaugucuauauccTT-3′
siRNA-unrelated control:	5′-agugguaaugucuauauccTT-3′
siRNA SOD1:	5′-gguggaaaugaagaaaguaTT-3′

Effect of siRNA on expression and function of recombinant OAT3 in culture cells

siRNA OAT3 #2 most effectively reduced the expression of OAT3 in HEK293 cells by 86.2% on luciferase activity compared with control siRNA with shuffle sequence of siRNA OAT3 #2 (Fig. 1). siRNA OAT3 #1 and #3 were moderately effective.

To investigate the inhibition effect of siRNA OAT3 to its efflux function in vitro, we measured uptake of OAT3 substrate, [^{3}H]benzylpenicillin. After expression of OAT3

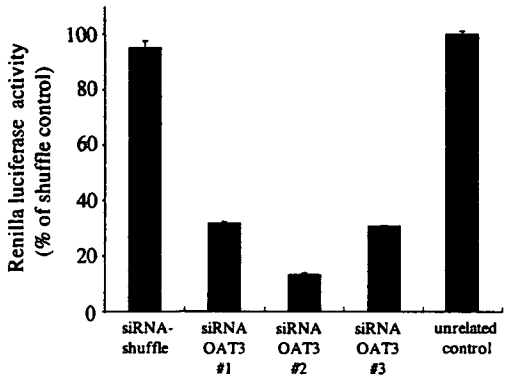

Fig. 1. Effect of siRNAs directed against the OAT3 in vitro. HEK293 cells were transfected with *Renilla* luciferase-fused OAT3 expression vector, *firefly* luciferase expression vector, and 25 nM siRNA. Reduction effect of *Renilla* luciferase activity relative to *firefly* luciferase activity was analyzed. Negative controls were the siRNA with randomized sequence of siRNA OAT3 #2 (siRNA-shuffle) and the siRNA against unrelated gene. Data were averaged from three experiments with SEM indicated.

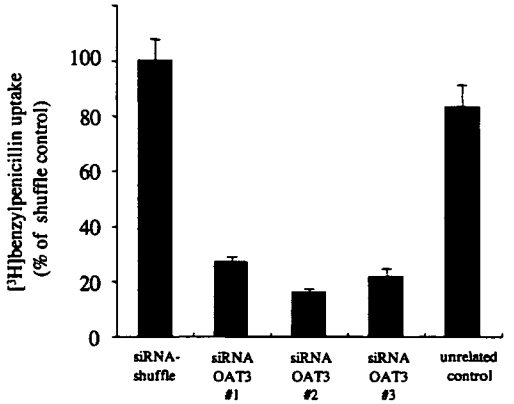

Fig. 2. Effect of siRNAs on uptake of OAT3 substrate in culture cells. Effect of siRNAs OAT3 on the OAT-3-mediated [^{3}H]benzylpenicillin uptake in HEK293 cells. After expression of OAT3 to the cells, [^{3}H]benzylpenicillin uptake was performed at 2 min, reflecting the initial uptake phase. All siRNAs were used at a concentration of 100 nM. Each value represents the mean ± SEM ($n = 4$). The increased uptake by expression of OAT3 was significantly reduced by siRNA OAT3 compared to siRNA-shuffle and siRNA-unrelated control. ($p < 0.0001$).

to HEK293 cells, the uptake mediated OAT3 was increased, and siRNA OAT3 #2 significantly inhibited the increased uptake of the substrate in HEK293 cells, compared with siRNA-shuffle and siRNA-unrelated control (Fig. 2).

In vivo delivery of siRNA to brain endothelial cells

We biochemically investigated an inhibitory effect of siRNA on expression of endogenous protein in BCECs using brain vascular fraction of small vessels from mouse brain.

For detection of endogenous protein in BCECs, we used SOD1 and siRNA to SOD1, because we have confirmed the efficient in vivo effect of this siRNA to endogenous mouse SOD1 in the siRNA-overexpressed transgenic mouse [14].

Western blot of the mouse brain small vascular fraction showed a reduction of endogenous mouse SOD1 level after hydrodynamic injection of siRNA SOD1 (Fig. 3A, left), whereas SOD1 level in the total homogenate of brain did not change (data not shown). There was a potentially more significant level of reduction on a per-BCEC basis, because the brain small vascular fraction contained proteins from cells other than BCECs such as pericytes and astrocytes [15]. We roughly estimated the content of BCECs in the brain small vascular fraction by performing a Western blot analysis with antibody to glucose-transporter-1 (GLUT-1) which specifically expressed in BCECs (Fig. 3B). The band intensity of GLUT-1 in the brain small vascular fraction was 4.1 (± 0.58) times more than that in mouse brain capillary endothelial cell lines which we previously established [12] (Fig. 3B). Since the cell line contains more than 1/8 of GLUT-1 [12], around 50% protein of the brain small vascular fraction that we made was supposed to come from brain endothelial cells.

In contrast, there was not obvious reduction of SOD1 level in the small vascular fraction after a regular intrave-

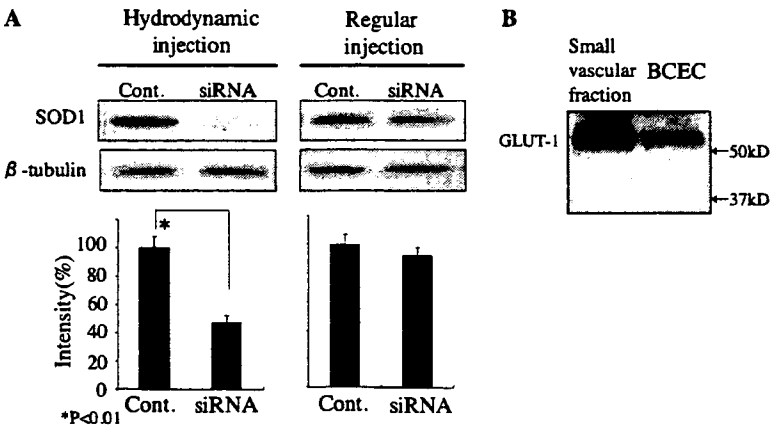

Fig. 3. Western blot analysis of mouse brain capillary-rich fraction. (A) The mouse brain small vascular fraction was examined on Western blot analysis after hydrodynamic (left) and regular (right) injection of 50 μg siRNA SOD1. The lower panels indicate percentages of signal intensities of SOD1 normalized with that of tubulin. (B) Western blot analysis with 2.5 μg protein of anti-GLUT-1 antibody of the mouse brain small vascular fraction (left) and mouse brain capillary endothelial cell lines (right). Signal intensity of GLUT-1 in the mouse brain small vascular fraction is 4.1 (± 0.58) times more than that in mouse brain capillary endothelial cell lines. BCEC, brain capillary endothelial cell line cells.